1-1-2019

Capturing Transmission and Distribution Connected Wind Energy Variability

Abdulaziz Alanazi
University of Denver

CAPTURING TRANSMISSION AND DISTRIBUTION CONNECTED WIND ENERGY VARIABILITY

A Dissertation

Presented to

the Faculty of the Daniel Felix Ritchie School of Engineering and Computer Science

University of Denver

In Partial Fulfillment

of the Requirements for the Degree

Doctor of Philosophy

---

by

Abdulaziz Alanazi

August 2019

Advisor: Dr. Amin Khodaei

Author: Abdulaziz Alanazi
Title: CAPTURING TRANSMISSION AND DISTRIBUTION CONNECTED WIND ENERGY VARIABILITY
Advisor: Dr. Amin Khodaei
Degree Date: August 2019

Abstract

Although renewable energy provides a viable solution to address ongoing challenges of the economy and the environment in modern power systems, the variable generation of this technology results in major technical challenges for system operators. This issue is becoming more severe as the penetration of renewable generation is increasing. This dissertation addresses the variability challenge of renewable energy resources in transmission and distribution levels of modern power systems.

For transmission level, this dissertation focuses on wind generation fluctuation. Three methods of reducing wind generation fluctuation are investigated from an economic perspective, including (a) dumping the wind generation, (b) using battery energy storage system (BESS) to capture excess wind generation, and (c) a hybrid method combining these two approaches. The economic viability of the hybrid method is investigated via a developed linear programming model with the objective of profit maximization, which in extreme cases will converge to one of the other methods. This dissertation further proposes a BESS planning model to minimize wind generation curtailment and accordingly maximize the deployment of this viable technology.

For distribution level, this dissertation investigates the issue of microgrids net load variability stemmed from renewable generation. This is accomplished by investigating and comparing two options to control the microgrid net load variability resulted from high penetration of renewable generation. The proposed options include (a)

Local management, which limits the microgrid net load variability in the distribution level by enforcing a cap constraint, and (b) Central management, which recommends on building a new fast response generation unit to limit aggregated microgrid net load variability in the distribution level. Moreover, the aggregated microgrid net load variability is studied in this dissertation by considering the distribution system operator (DSO). DSO would calculate the microgrids net load in day-ahead basis by receiving the aggregated demand bid curves. Accordingly, two models are proposed considering the DSO role in managing the grid operation and market clearing. The first one is security-constrained distribution system operation model which maximizes the system social welfare. The system security consists of distribution line outage as well as microgrid islanding. None of these two security events are in the control of the DSO, so associated uncertainties are considered in the problem modeling. The second one aims at reconfiguring the distribution grid, i.e., a grid topology control, using the smart switches in order to maximize the system social welfare and support grid reliability.

The conducted numerical simulations demonstrate the effectiveness and the merits of the proposed models in identifying viable and economic options in capturing renewable generation variability.

Acknowledgments

It is a privilege to work with my wonderful advisor Dr. Amin Khodaei. It is an amazing and unforgettable experience in my life. He is a very supportive and helpful professor. A lot of challenges and obstacles were overcome by his support and guidance. Here it is the time to thank him for all of his advising and assistance, which really helped me in my research and really improved my knowledge in my research area.

It is my honor to have this grateful committee members, Dr. David Wenzhong Gao and Dr. Mohammad Matin, who provided me with valuable observations, feedback and comments on my PhD dissertation. Moreover, I want to send my best regards to the external committee member, Dr. Andy Goetz, for giving me some of his time and serving as chair of my oral defense committee.

Last but not least, I should not forget to thank all my colleagues in the K-Lab since they have provided me with all support and information which assisted me in my research during my Ph.D. I also extend my deep thanks to the Northern Border University who granted me this chance to pursue my Ph.D by supporting me financially.

Finally, I dedicate this work for my wonderful parents (Furreh and Shema), my lovely wife (Ohud) and my kids (Meshari, Danah, and Kadi) as they assisted and support me to finish my degree and overcame all challenges.

Table of Contents

List of Figures

List of Tables

Nomenclature

Chapter two

Indices:

ch	Subscript for BESS charging
dch	Subscript for BESS discharging
d	Index for day
t	Index for hour

Parameters:

B	Maximum investment budget
ECC	Annualized energy rating capital cost
$E^{b,\max}$	Maximum BESS energy rating
$E^{b,\min}$	Minimum BESS energy rating
k	Battery life cycle
L	Limit of the generated wind power
$P^{b,\max}$	Maximum BESS power rating
$P^{b,\min}$	Minimum BESS power rating
PCC	Annualized power rating capital cost
P^{w}	Generated wind power
ρ	Electricity market price
η	BESS efficiency

Variables:

D	Dumping amount of wind power
E	BESS hourly stored energy
E^{b}	BESS rated energy
P^{b}	BESS rated power
P	BESS hourly output power
u	BESS discharging state
v	BESS charging state

Chapter three

Indices:

i	Index for dispatchable units
l	Index for lines
m	Index for buses
t	Index for time

Parameters:

CE	Annualized energy rating capital cost

CP	Annualized power rating capital cost
D	BESS depth of discharge
$E^{R,\max}$	Maximum BESS energy rating
$E^{R,\min}$	Minimum BESS energy rating
$F(.)$	Generation cost
IB	Maximum investment budget
k	Battery life cycle
$P^{\max}$	Maximum limit of units' generation
$P^{\min}$	Minimum limit of units' generation
$P^{R,\max}$	Maximum BESS power rating
$P^{R,\min}$	Minimum BESS power rating
P^{w}	Generated wind power
PD	Demand power
PL^{max}	Maximum capacity for transmission lines
α	Linear sensitivity factor
ρ	Electricity market price
η	BESS efficiency

Variables:

C^{w}	Curtailed amount of wind generation
E^{B}	BESS stored energy
E^{R}	BESS rated energy
P	Units generated power
P^{R}	BESS rated power
P^{ch}	BESS charging power
P^{dch}	BESS discharging power
P^{B}	BESS output power
P^{G}	Net injection power at each bus
PL	Power flow for each line
u	BESS charging state
v	BESS discharging state

Chapter four

Indices:

D	Index for day
i	Index for dispatchable units
t	Index for time

Parameters:

C	Generation cost coefficient
CSD	Shut down cost
CSU	Startup cost
D	Load demand
FC	Fixed O&M cost

GPC	Gas power plant capacity
H	Number of hours
k	Variability cap
MD	Minimum down time
MF	Number of hours the unit can be OFF
MN	Number of hours the unit can be ON
MU	Minimum up time
NL	No load cost
OCC	Overnight capital cost
P^{max}	Maximum generation capacity
P^{min}	Minimum generation capacity
PBP	Payback period
P_M^{max}	Capacity of transmission line between the utility and the microgrid
RD	Ramp down rate
RU	Ramp up rate
VC	Variable O&M cost
W	Wind power
ρ	Market price

Variables:

I	Commitment state of the dispatchable units
P	DER generated power
P_M	Microgrid net load
sd	Number of successive OFF hours
su	Number of successive ON hours
TC	Total operation cost
y	Startup indicator
z	Shut down indicator

Chapter five

Indices:

c	Index for POI
i	Index for microgrids
j	Index for microgrids bid segments
m, n	Index for buses
s	Index for scenarios
t	Index for time
^	Index for calculated variables

Sets:

B	Set of buses
B_m	Set of buses adjacent to bus m
C_m	Set of POIs at bus m
D_m	Set of microgrids connected to bus m

L	Set of lines
L_i	Set of lines connected to microgrid i

Parameters:

a	Elements of the incidence matrix
b	Line susceptance
g	Line conductance
M	Large positive number
$P^{M,max}$	Capacity of real power transfer to the distribution network
$P^{MG,D}/Q^{MG,D}$	Microgrid fixed real/reactive power demand
$P^{MG,max}/Q^{MG,max}$	Microgrid real/reactive power capacity
PD/QD	Fixed real/reactive power demand in buses without microgrid
PL^{max}/QL^{max}	Maximum real/reactive power flow for distribution lines
PX^{max}	Maximum limit for each demand segment
RR	Ramp rate of each bid segment
w	Distribution lines outage state
λ^{T}	Transmission locational marginal price (T-LMP).
ϑ^{P}	Value of lost real load
ϑ^{Q}	Value of lost reactive load

Variables:

$B(.)$	Load benefit function
I	Microgrid islanding state
PS/QS	Real/reactive power load curtailment
P^{M}/Q^{M}	Real/reactive power transfer from the ISO
$P^{MG,net}/Q^{MG,net}$	Real/reactive power transfer between the utility and the microgrid
PL/QL	Real/reactive power flow
PX	Real power for each demand segment
RR^{sel}	Selected ramp rate of each microgrid
V	Bus voltage magnitude
θ	Bus voltage angle
δ	Binary state variable of the selected bid segment

Chapter One: Introduction

The renewable energy is expected to lead the future of energy generation as the governments in developed countries encourage to increase the renewable installations via offering incentives and setting renewable mandates to increase penetration and reap the benefits of this viable and environmentally-friendly technology. In the United States many incentives and regulations can be found for this purpose, including but not limited to environmental regulations, interconnection standards, net metering policy, feed-in tariffs, and property assessed clean energy [1]–[4]. In some countries, the existing renewable energy capacity exceeds 40% of the total installed capacity [5]. Wind energy has the largest installed capacity worldwide among other renewable resources. In case of wind turbine technology, the focus is on both offshore wind generation, as well as onshore generation [6], which is boosted by recent improvements in wind energy technology and increased net benefits [7], [8]. In 2017, the cumulative installed wind generation capacity reached 539.6 GW up from 487.7 GW in 2016 with an increase of 10.65%[9], [10]. The global growth of wind generation capacity is shown in Fig. 1.1. Wind energy is considered a viable energy resource to use as it is clean and inexpensive, however, it poses several challenges when it comes to grid integration. One of the challenges is that wind generation is variable and uncontrollable [11]. In other words, it is subject to volatility (constant fluctuations) and intermittency (frequent unavailability),

which makes integration and operation of this viable energy resource to the power grid a difficult task for system operators in order to make the power system stable and balanced. This issue will be more severe as the wind penetration increases in the system, and the drawback will be seen by both system operators and wind farm owners [12]. Moreover, this high penetration of wind generation makes wind integration a difficult task as it affects various aspects of the power system operation such as power quality, stability, and economics [13].

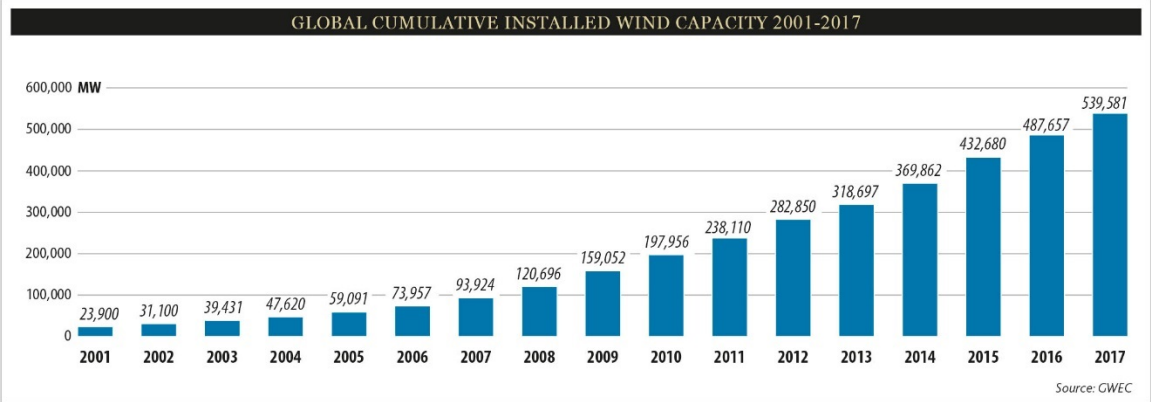

Fig. 1.1 Global cumulative installed capacity of wind generation **[10]**

The second challenge in wind integration, which is more economical than technical, is the large capital cost associated with the technology, although offering extremely low operation costs. Considering this, wind turbines are commonly operated on maximum power point tracking (MPPT), so the payback period is reduced [14], [15]. When a wind turbine is connected to the grid, the injected wind generation into the grid must follow the power grid's standards [16], which are followed and complied by all generation resources in the grid. Therefore, the highly fluctuating wind power has to be smoothed to its allowable limits from a power system operator's perspective. This reduction in fluctuations, however, should be carried out while taking the economic

benefits of the wind farm owners into consideration [17]. In [18], authors found that uncertain wind power variations must be compensated by units with fast generation response, for example natural gas or hydro, to ensure system/nodal power balance and to maintain grid stability. The California Independent System Operator (CAISO) has conducted a study and found that the variations in renewable generation can cause significant issues in power system supply-demand balance. The supply-demand imbalance causes oversupply risk, mainly in morning hours when the load demand is low while the wind generation is high. Therefore, it is required to increase the system elasticity using fast up or down ramping, see Fig. 1.2 [19].

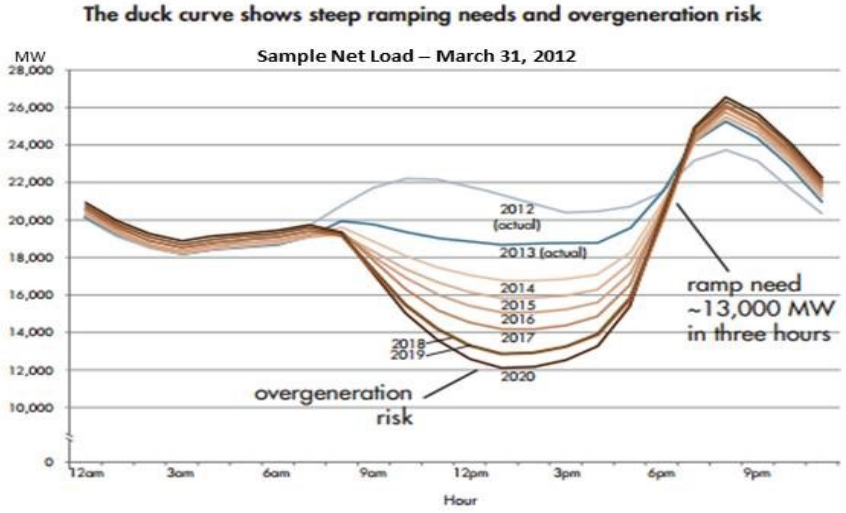

Fig. 1.2 The California ISO duck curve [19]

Although an aggregation of wind turbines (i.e., wind farm) would result in less variable output, the generation fluctuations would still be noticeable and significant in power system operation [20]. The study in [21] proposes to equip wind turbines with a control system for inertial power smoothing in a frequency range of 0.01 Hz or higher. It is found that the losses of wind power at these frequencies will not exceed 1.5% regardless of the wind speed. In addition, the power electronics can be used to smooth the

wind power fluctuations but these methods may reduce the power produced by the wind turbines [22]. Additional studies found that various types of the storage systems could shape the wind turbine output power to the desired profile. In [23], another approach is proposed to smooth a large scale wind farm power, suggesting the conversion of conventional parking lots to smart parking lots, thus to create a huge charging and discharging capacity That can be used for reducing renewable generation fluctuations.

This dissertation focuses on capturing energy variability in modern power systems at both transmission (large-scale) and distribution (small-scale) levels. The large-scale integration include renewable energy resource in transmission level which ranges in 10s of MWs [24], where variability could be as large as 70% of the installed capacity in 5 to 10 minutes [25]. The small-scale integration comprises renewable energy resource in distribution networks, and particularly within microgrids, which may cause microgrids net load variability in distribution level.

1.1 Reducing Wind Power Variability in Transmission level

There are many methods are proposed to reduce the power fluctuation while wind turbines generate the maximum power, such as dumping wind power [26], using pumped hydro storage system [27] and having energy storage systems [4]. These methods can help with the grid stability and reliability while ensuring maximized economic benefits for the wind farm owners and developers. In chapter two, a new hybrid model is proposed to address the wind power fluctuation reduction. This model joins two methods together: 1) the first one is dumping any excess power over the utility-imposed limit and 2) the second one is to use a BESS. The developed hybrid model determines the optimal size of the BESS as well as the amount of wind generation that needs to be dumped.

Despite that it is imperative to curtail wind generation at some strategic points of the system under these conditions, it is deemed less desirable and considered as a loss for both system operator and the wind farm owners. Wind generation curtailment is defined as reduction in wind generation from what it could generate, or in other words, the amount of wind generation that the system operator is unwilling to inject into the network [14]. Wind generation curtailment has been practiced in many electricity markets inside and outside the United States. Some examples and practices as well as the main reasons behind curtailment are found in [14], [28]–[30]. Fig. 1.3 shows the curtailment level that occurred in some electricity markets inside the United States from 2007 to 2013. Most of curtailments were ranged from 1% to 4% of the total wind generation. However, in some areas, such as in ERCOT territory, wind generation curtailments as high as 17% were recorded. Wind generation curtailment has also occurred in New England ISO (NE-ISO) and CAISO, which are not mentioned in Fig. 1.3. NE-ISO reduced wind generation capability of a 45 MW wind unit in Vermont NE to only 20 MW [31]. In 2017, CAISO curtailed 60 GWh and 80 GWh of wind generation in February and March, respectively, up from 21 GWh and 47 GWh in the corresponding months of the previous year [32]. The reasons of wind generation curtailment vary from market to market, but the common reasons are the lack of adequate transmissions capacity to transmit the generated power (i.e., under transmission congestion), and the simultaneous oversupply of wind generation with low load.

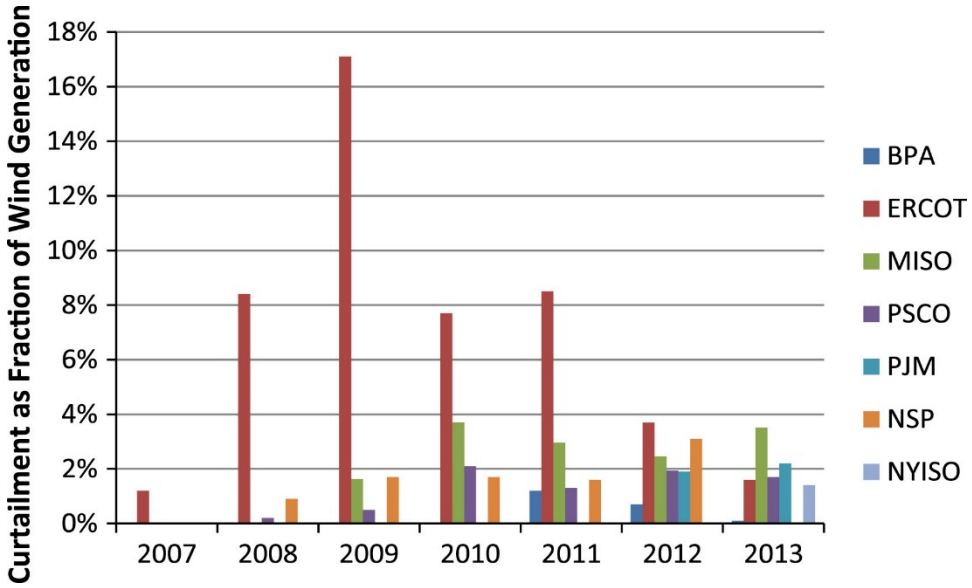

Fig. 1.3 The wind generation curtailment in the U.S. by electricity market **[14]**

The massive wind generation curtailment experiences mentioned above show an increase in energy waste. However, it is crucial to curtail the wind generation to acceptable levels under some operating conditions, such as oversupply. In [33], authors present applications of wind curtailment reduction in different countries. Reducing the wind generation curtailment can be accomplished by increasing the power system flexibility through installation of BESS. The excess wind generation can be stored in BESS by the charging process for later used by discharging when wind generation is low. In chapter three, a planning model is proposed to reduce the wind generation curtailment. The main objective is to find the optimal amount of wind generation curtailment that allows an efficient integration in the power system, as well as the optimal size of the BESS which helps to save some or the entire curtailed amount of wind generation.

1.2 Managing Net load Variability in Distribution level

Chapter four proposes a model to address the challenge of integrating renewable generation in microgrids. One reason of microgrids net load variability is integration of renewable energy resources into in a small-scale power system, such as microgrids. Since wind energy has the largest installed capacity among renewable energy resources, as mentioned above, this dissertation focuses on its variability in distribution level as well. In [34], a study of integrating wind generation within a microgrid is conducted. The study proposes operational controls to help with the wind integration and managing the wind generation variability. Wind energy, as mentioned above, is rapidly growing in power systems, primarily due to the falling cost of the technology and strict environmental mandates. The wind generation variability, however, has presented a significant challenge in ensuring a reliable supply-demand balance when utilizing this technology in microgrids. As the penetration of wind generation increases in the microgrid and there is a high microgrid penetration in the utility grid, the wind generation variability may cause a severe negative impact on the microgrid net load from utility's perspective.

Consequently, it is worth to study the increase of microgrids penetration in distribution level and investigate their impact on distribution market. Microgrids help to increase the distribution system reliability and resiliency by allowing consumers to partially or fully supply their demand [35], while at the same time add technical complexity to grid management. Microgrids, as advanced technologies that integrate and manage several DERs and loads, are also responsive to day-ahead price signals which leads to microgrids net load variability [36]. In either case, it has become evident that a distribution system operator (DSO) to manage the local distribution grid and solve this

added complexity in a local manner is necessary. The DSO offers many advantages for the distribution system such as increasing the participation of proactive customers and allowing them to play a direct role in the electricity market, removing the uncertainty of proactive loads, and further reducing the required two-way communications between the ISO and proactive customers by forming an intermediate point of contact.

Distribution system operators (DSOs) will play an important role in future power grids to incentivize and increase the participation of proactive customers in distribution electricity markets, and accordingly, address many operational challenges caused by the growing proliferation of such customers [37]. In the past few years, there has been a growing interest in studying various DSO models to help transform the distribution system operations. Examples in the U.S. are the concept of Distribution System Platform Provider (DSPP) in New York introduced through Reforming the Energy Vision (REV) program [38], the DSO concept proposed in California [39], and the idea of transforming the utility to a platform business model proposed by ComEd in Illinois [40], to name a few. Additional models have also been discussed, including but not limited to Distribution Network Operator (DNO) [41], Distribution Market Operator (DMO) [42], and Independent distribution system operator (IDSO) [43].

Despite different terminologies, existing models share a somewhat similar definition for the DSO, i.e., an independent entity placed between the proactive customers and the ISO to streamline customers' participation in the electricity market as well as to coordinate with the electric distribution company to enhance grid operations [44]. This dissertation, furthermore, proposes two models considering DSO, chapter five proposes a security-constrained distribution system market clearing model while chapter

six focuses on maximizing the social welfare in the distribution market through grid reconfiguration.

Chapter Two: Wind Power Variability Reduction in Transmission Level

2.1 Introduction

In this chapter, two methods are studied to address the variable wind generation [45]. The first one is dumping any excess power over the utility-imposed limit. The second one is to use a BESS. The main objective of these methods is to make the wind generation smoother (i.e., less variable), and to some extent, dispatchable. Both methods are investigated through a developed hybrid model that can simultaneously accounts for both methods using an economic viability approach in which the investment cost of the BESS is compared with the lost revenue from dumping wind generation. The developed hybrid model determines the optimal size of the BESS as well as the amount of wind generation that needs to be dumped. This method further has the capability to select only one of these two methods if the other one is deemed less desirable in terms of ensuring economic benefits.

2.2 Wind Power Smoothing Model Outline and Formulation

The main objective of the proposed model is to find a method that helps smooth the wind power fluctuations to meet the utility grid limits while maximizing economic benefits from selling wind generation to the grid. The proposed model combines two different methods of wind power dumping (power curtailment) and the BESS application. For wind power dumping, some power electronics is applied to avoid generated power

having big fluctuations when the wind speed increases, but when the wind speed decreases, the power electronics cannot help (power electronics can help dump power but it cannot generate power or store energy). The advantage of this method lies in the small capital cost or maintenance cost as no additional equipment needs to be installed and coordinated with the wind turbine. Depending on the fluctuations, BESS can be used to reduce the power fluctuation by properly charging and discharging energy, i.e., shifting the excess generations to other hours with relatively lower generation. However, the BESS imposes an investment cost which needs to be carefully considered in studies. The proposed hybrid model considers both these methods at the same time and offers the capability to select a combination of the two methods. The BESS budget constraint is added to impose a specific budget that cannot be exceeded. All costs and prices in this model are annualized. The proposed formulations are modeled using a Mixed-Integer Linear Programming (MILP) approach.

The objective function is proposed as in (2.1) which seeks to maximize the total annual profit of the wind farm owner. This profit is presented as the cost of wind generation minus the BESS investment cost.

$$\max\left[\sum_{t}\sum_{d}\rho_{td}\left(P_{td}^{w}-D_{td}^{w}\right)-\left(P^{b}PCC+E^{b}ECC\right)\right] \tag{2.1}$$

$$P^{b,\min}\le P^{b}\le P^{b,\max} \tag{2.2}$$

$$E^{b,\min}\le E^{b}\le E^{b,\max} \tag{2.3}$$

$$0\le P_{td}^{dch}\le P^{b}u_{td} \qquad \forall t,\forall d \tag{2.4}$$

$$-P^{b}v_{td}\le P_{td}^{ch}\le 0 \qquad \forall t,\forall d \tag{2.5}$$

$$E_{td} = E_{t-1,d} - \frac{P_{td}^{dch}}{\eta} - P_{td}^{ch} \qquad \forall t > 1, \forall d \qquad (2.6)$$

$$E_{1,d} = E_{24,d-1} - \frac{P_{1,d}^{dch}}{\eta} - P_{1,d}^{ch} \qquad \forall d > 1 \qquad (2.7)$$

$$0 \le E_{td} \le E^{b} \qquad \forall t, \forall d \qquad (2.8)$$

$$u_{td} + v_{td} \le 1 \qquad \forall t, \forall d \qquad (2.9)$$

$$\sum_{t}\sum_{d} u_{td} \le k \qquad \forall t, \forall d \qquad (2.10)$$

$$P_{td}^{w} + P_{td}^{dch} + P_{td}^{ch} - D_{td}^{w} \le L \qquad \forall t, \forall d \qquad (2.11)$$

$$P^{b}PCC + E^{b}ECC \le B \qquad (2.12)$$

The first term in the objective (2.1) represents the profit of wind power which is always positive and is considered as an income as the wind energy is sold by the wind farm to the utility grid. The second and third terms represent the BESS investment cost which includes BESS power and energy capital costs, respectively. The BESS sizing is modeled by (2.2) and (2.3) by restricting the power and energy ratings between minimum and maximum values. The BESS charging and discharging powers are modeled by (2.4) and (2.5). The charging power is always negative since it is considered as a load, whereas the discharging power is positive as it is considered a generation source. The stored energy in the BESS is calculated for each hour via (2.6)-(2.7) and is constrained by (2.8). Constraint (2.7) calculates the stored energy at hour 1 of each day (based on the stored energy at hour 24 of the previous day), while (2.6) calculates the stored energy for other hours of the day. The stored energy is calculated as the stored energy at the previous hour

minus the amount of charged/discharged power. Since the charging power is considered as a negative variable, the stored energy will increase when the BESS is charging. The BESS charging/discharging efficiency is considered by adjusting the discharged power. The charging and discharging states are represented by binary variables v and u, respectively. The binary discharging indicator u equals 1 when the BESS is discharging otherwise it is 0. Similarly, the binary charging indicator v equals 1 when the BESS is charging, otherwise 0. It is made sure that these two binary variables are not 1 at the same time using (2.9). A battery life cycle constraint (2.10) is imposed on the BESS charging/ discharging cycles to prolong the battery lifetime. The net output power of the combined wind farm and the BESS, which is defined as the summation of the wind power and the BESS net power, is calculated and ensured that it does not violate the utility-imposed limit (2.11). This limit ensures that the combined wind power and BESS power will not exceed the imposed limit, hence the variability in wind power will be captured by the BESS whenever necessary, and thus the fluctuations will be mitigated. A dumping variable is further added to this constraint to determine the optimal amount of hourly dumping if necessary. The wind generation dumping appears as a load, or as shown in (2.11), a negative generation. The impact of the generation dumping is further reflected in the objective (2.1). Finally, the BESS budget constraint is modeled by (2.12) to ensure that the investment cost does not exceed the available budget.

The outcome of this optimization problem will be three variables: the optimal BESS rated power (P^b), the optimal BESS rated energy (E^b), and the amount of hourly dumping (D^w_{td}). If the first two are zero, it means that the generation dumping is the most

economical solution, while if last variable is zero, it means that the BESS installation was successful in fully capturing all fluctuations over the imposed limit. As discussed, a solution in between is also possible which represents that both methods are required to be utilized at the same time to ensure highest possible economic benefits.

2.3 Numerical Simulations

The proposed hybrid wind power-smoothing model is applied to a test wind farm with an aggregated capacity of 14 MW. One-year time horizon of forecasted wind power data and market price data are used in the studies. The BESS characteristics are selected and presented in Table 2.1. The proposed MILP model is utilized to solve the following cases:

Case 1: Base case (dumping the wind power without adding the BESS)

Case 2: Using a fixed BESS capacity

Case 3: Solve the optimization model to find the optimal BESS size and generation dumping for the wind farm

Table 2.1: BESS Characteristics

Maximum Power rating (MW)	Maximum Energy rating (MWh)	Power rating capital cost ($/MW/yr)	Energy rating capital cost ($/MWh/yr)	BESS efficiency (%)
10	20	20,000	11,000	90

Case 1: In this case the wind generation is dumped whenever necessary to meet the utility-imposed limit. A sample one-week data of the wind power profile is shown in Fig. 2.1. The imposed limit is selected as 6 MW. The total profit of the base case is calculated before and after dumping the power is calculated, in which the difference would represent the lost revenue. The total profit without the limit is calculated as

$5,825,912, which is reduced to $5,173,639 after imposing the limit and dumping generation. The lost revenue is calculated as $652,273. Despite the large lost revenue, which represents more than 11% of the initial profit, the wind power has to be dumped since the fluctuations can potentially harm the power system. The overall dumped energy is 4470 MWh for this case. Fig. 2.2 shows the dumped wind power profile for one week. The red line is sold wind generation to the utility grid which is less variable but considerably lower than the maximum generated wind power in many hours.

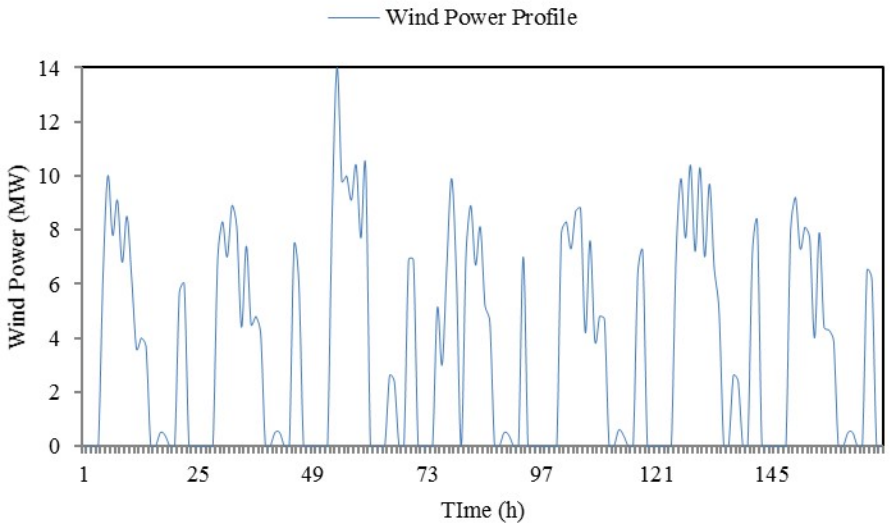

Fig. 2.1 Wind power profile for one sample week

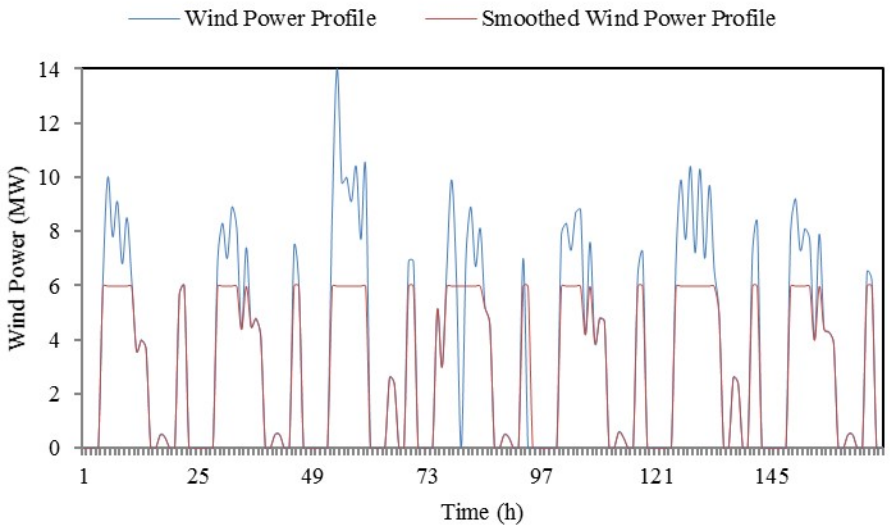

Fig. 2.2 Smoothed wind power by dumping wind power (Case 1)

Case 2: In this case a fixed BESS capacity, regardless of the wind power fluctuation, is added to the wind farm. The fixed BESS capacity is selected to be 5 MW and 10 MWh for rated power and rated energy, respectively. The imposed limit is still selected to be 6 MW to enable comparisons. Using this BESS, the wind power profile will be smoothed as shown in Fig. 2.3, but it may not represent the optimal solution. The total profit is $5,220,632 which represents an increase of approximately 0.91% compared to Case 1. By using fixed BESS, the total dumped energy is reduced to 3349 MWh. This result advocates that using BESS has increased the total wind farm profit and while considerably improved the wind power profile.

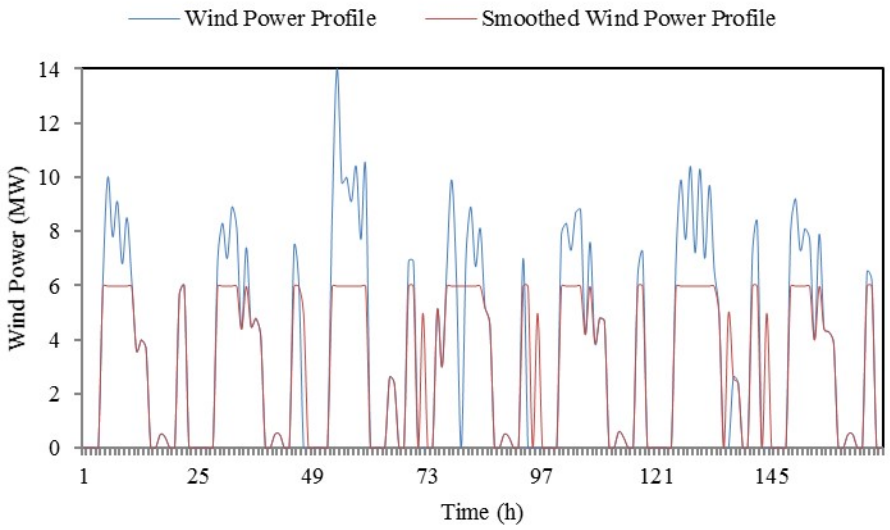

Fig. 2.3 Smoothed wind power by fixed BESS capacity (Case 2)

Case 3: The proposed optimization model to find a hybrid solution is studied in this case, which would find the optimal BESS capacity and the amount of dumped generation. The optimal capacity of BESS in this case is calculated as 2.7 MW for rated power and 3 MWh for the rated energy. The total profit of the wind farm is calculated as $5,263,126, which is the highest profit among the three studied cases and is more than 1.73% of the profit in Case 2. The dumped energy is calculated as 3939 MWh. The wind power fluctuations are also less than the other two cases as shown in Fig. 2.4.

Table 2.2: Summary of Studied Cases

	Total profit ($)	BESS cost ($)	Cost of dumped generation ($)
Case 1	5,173,639	0	652,273
Case 2	5,220,632	210,000	395,280
Case 3	5,263,126	87,000	475,786

Table 2.3: The Fluctuation Reduction Based on Standard Deviation In Studied Cases

Original wind profile	Studied cases	
3.412	Case 1	2.738
	Case 2	2.725
	Case 3	2.705

Table 2.2 summarizes the results of these three cases, including the total profit, BESS cost, and total dumped generation. To measure the variability improvement for each case, the standard deviation is calculated and listed in Table 2.3, where smaller standard deviations represent less fluctuation. As presented, the Case 3 solution ensures less fluctuations compared to other two cases.

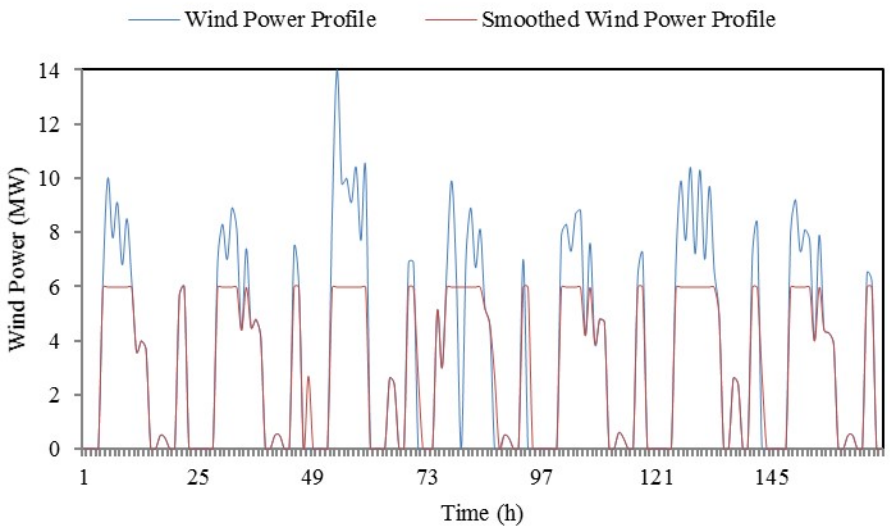

Fig. 2.4 Smoothed wind power profile by optimal BESS capacity (Case 3)

The impact of the utility-imposed limit on the BESS rated power and rated energy is further analyzed and shown in Fig. 2.5 and Fig. 2.6, respectively. It is clear that when the limit is increased, the BESS capacity decreases and vice versa. In addition, it can be concluded from these figures that using only the dumping wind power method is more economical than using hybrid method when the limit more than 6 MW. Otherwise, it is more beneficial to use the proposed hybrid method when the limit is less than or equal 6 MW.

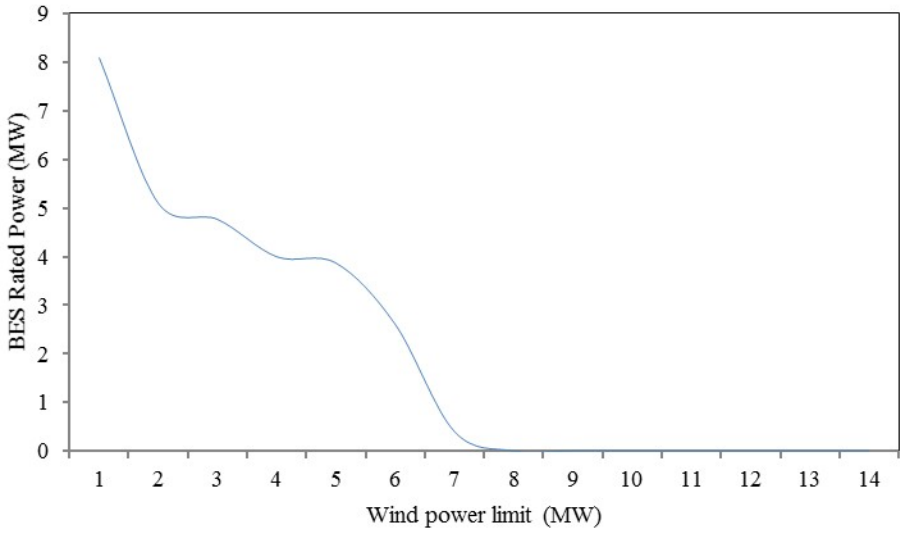

Fig. 2.5 Impact of wind power limit on BESS rated power

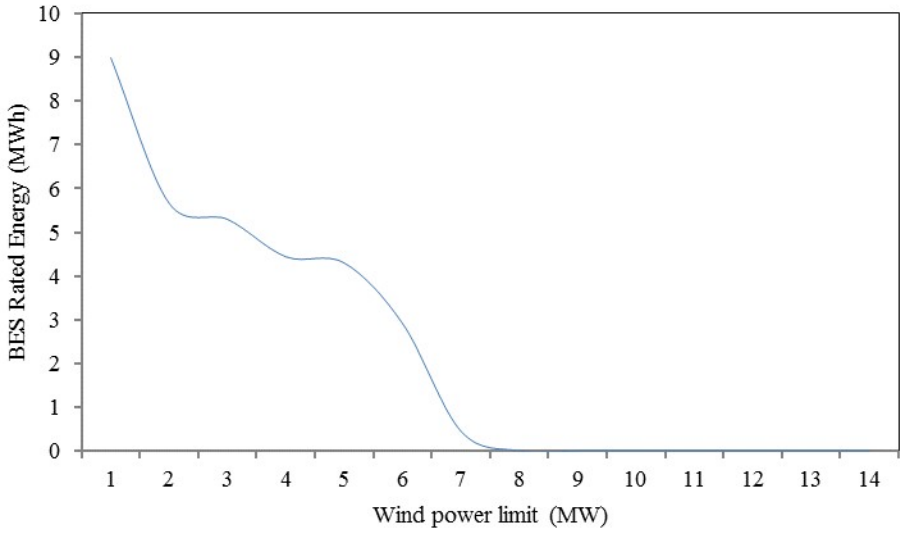

Fig. 2.6 Impact of wind power limit on BESS rated energy

Chapter Three: Optimal Battery Energy Storage Sizing for Reducing Wind Generation Curtailment

3.1 Introduction

In this chapter, a planning model is proposed to reduce the wind generation curtailment [46]. Despite the benefits of wind generation curtailment to make the power system stable and balanced, it is deemed less desirable since the wind generation is inexpensive and the curtailment is considered a loss for both the system and the wind farm owner/developer. The proposed planning model is using a BESS to reduce and minimize the wind generation curtailment by storing the curtailed power and use it again at other operation hours when wind generation is low or the transmission network is not congested [45], [47]–[50]. The main objective of the proposed planning problem is to find the optimal amount of wind generation curtailment that allows an efficient participation in the system, as well as the optimal size of the BESS which helps to save some or the entire curtailed amount of wind generation.

3.2 Wind Generation Curtailment – Model Outline and Formulation

The proposed planning model seeks to maximize the economic benefits of the wind generation. This objective is achieved by simultaneously minimizing the investment cost of the BESS (that is an optimal sizing problem) along with minimizing the amount of curtailed wind generation. To curtail the wind generation, power electronics devices

are used which would prevent overgeneration whenever the curtailment is needed. The BESS is used to reduce the wind generation curtailment by properly charging and discharging energy, i.e., shifting the surplus generation to other low wind generation hours. The BESS budget constraint is further considered to maintain a certain investment budget that cannot be surpassed. The model is developed based on annualized costs. The objective function is proposed in (3.1) which minimizes the total annual system operation cost, considering the wind generation curtailment, plus the BESS investment cost. The first term in (3.1) represents the operation cost of units and the second term denotes the BESS investment cost.

$$\min \sum_{i} \sum_{t} F_i\left(P_{it}\right) + \left(P^R CP + E^R CE\right) \tag{3.1}$$

The objective function is subject to a number of system operation (3.2)-(3.5) and BESS constraints (3.6)-(3.15).

3.2.1 Operation Constraints

The operation problem is formulated as an economic dispatch (3.2)-(3.5). Dispatchable units generation is limited between its associated maximum and minimum generation capacities (3.2). The power flow equation (3.3) determines the active power that flows in each transmission line. Transmission line flow is further limited to ensure the power flow in each line does not violate the transmission line capacity (3.4). The nodal load balance equation (3.5) ensures that the total generated power by generation units (dispatchable and renewable), plus the power of the added BESS equals the system total load demand. A positive variable for the wind generation curtailment is further added to (3.5) to determine the optimal amount of curtailment, if necessary.

$$P_i^{\min} \le P_{it} \le P_i^{\max} \qquad \forall i, \forall t \qquad (3.2)$$

$$PL_{lt} = \sum_m \alpha_{lm} P_{mt}^G \qquad \forall l, \forall t \qquad (3.3)$$

$$-PL_l^{\max} \le PL_{lt} \le PL_l^{\max} \qquad \forall l, \forall t \qquad (3.4)$$

$$\sum_i P_{it} + P_t^w + P_t^B = \sum_m PD_{mt} + C_t^w \qquad \forall m, \forall t \qquad (3.5)$$

3.2.2 BESS constraints

The BESS rated power and energy limits are modeled in (3.6) and (3.7), respectively, followed by discharging and charging powers in (3.8) and (3.9). The discharging power is always positive since BESS is producing power while it is discharging. Conversely, the charging power is negative as BESS is consuming power when it is charging. The BESS output power is the summation of BESS charging and discharging powers (3.10). The hourly BESS stored energy is calculated in (3.11) as the stored energy at the preceding hour minus the charged/discharged power, so the stored energy will increase when the BESS is charging (as the charging power is negative) and will decrease when the BESS is discharging (as the discharging power is positive). The stored energy is restricted by (3.12) considering the BESS depth of discharge. The charging and discharging states are denoted by binary variables *u* and *v*, respectively. The binary discharging state *v* is 1 when the BESS is discharging otherwise it is 0. The binary charging state *u* is 1 when the BESS is charging, otherwise it is 0. By using (3.13), it is ensured that both binary variables are not equal 1 at the same time (i.e., BESS is not charging and discharging simultaneously). A battery life cycle constraint (3.14) is applied on the BESS charging/discharging cycles to prolong the BESS lifetime. Furthermore, a

BESS budget constraint (3.15) is added to ensure that the investment cost does not surpass the available budget.

$$P^{\mathrm{R,min}} \le P^{R} \le P^{\mathrm{R,max}} \tag{3.6}$$

$$E^{\mathrm{R,min}} \le E^{R} \le E^{\mathrm{R,max}} \tag{3.7}$$

$$0 \le P_t^{dch} \le P^{R} v_t \qquad \forall t \tag{3.8}$$

$$-P^{R} u_t \le P_t^{ch} \le 0 \qquad \forall t \tag{3.9}$$

$$P_t^{B} = P_t^{dch} + P_t^{ch} \qquad \forall t \tag{3.10}$$

$$E_t^{B} = E_{t-1}^{B} - \frac{P_t^{dch}}{\eta} - P_t^{ch} \qquad \forall t \tag{3.11}$$

$$\left(1-D\right)E^{R} \le E_t^{B} \le E^{R} \qquad \forall t \tag{3.12}$$

$$u_t + v_t \le 1 \qquad \forall t \tag{3.13}$$

$$\sum_t v_t \le k \qquad \forall t \tag{3.14}$$

$$P^{R}CP + E^{R}CE \le IB \tag{3.15}$$

Solving the proposed optimization problem results in the optimal BESS size (P^R and E^R), and the amount of hourly wind generation curtailment ($C^w{}_t$). A zero value for the BESS size indicates that the wind generation curtailment is considered more economical than installing the BESS. However, if the optimal BESS size is non-zero, it can be concluded that the BESS is installed and it is capturing, partially or fully, wind generation.

3.2.3 The Robust Solution by Considering Wind Forecasting Uncertainty

The main objective of robust solution is to consider the uncertainty of wind generation forecast, and thus, to further ensure practicality of the obtained solutions. A robust optimization approach is applied to solve the problem under worst-case wind generation accuracy conditions [51]. The above proposed model will be modified to include the impact of forecasting error of wind generation. The objective function (3.1) of the above proposed model is modified to include robust optimization in (3.16). which minimizes the total annual system planning cost. The objective is simultaneously maximized to obtain the worst-case solution under the prevailing uncertainty of wind generation forecast.

$$\max_{\mathrm{U}} \min_{\mathrm{P}} \sum_{i} \sum_{t} F_i\left(P_{it}\right) + \left(P^R CP + E^R CE\right) \tag{3.16}$$

where i and t are the indices for dispatchable units and time, respectively. *F(.)* represents the operation cost function of dispatchable units. P is the amount of generated power by each unit. P^R and E^R are the BESS power and energy ratings. CP and CE are the annualized BESS investment cost for power and energy ratings, respectively. U and P are the uncertain parameters and primal variables, respectively. Uncertain parameters include the wind generation forecast and primal variables include the generated power by dispatchable units and the BESS size (i.e. rated power and energy variables). The robust optimization finds the worst-case solution as uncertain wind forecast varies within the uncertainty intervals. The worst-case solution is obtained by maximizing the minimum value of total planning cost over the uncertain parameter (i.e. the wind generation). The

robust solution ensures that the total planning cost is minimized based on the possible variation of the forecasted wind generation within its uncertainty interval.

The new objective function is subject to constraints (3.2)-(3.15), plus uncertainty constraint of wind generation forecast (3.17). Wind generation is obtained from the forecast and expanded within a range of uncertainty (i.e. a polyhedral uncertainty set). The range of uncertainty is the upper and lower limits that the wind generation forecast is expected to lie within [52].

$$P_t^w = \hat{P}_t^w + \overline{P}_t^w \overline{x}_t + \underline{P}_t^w \underline{x}_t \qquad \forall t \qquad (3.17)$$

$$\sum_t \left(\overline{x}_t + \underline{x}_t \right) \le \Gamma \qquad \forall t \qquad (3.18)$$

Considering a polyhedral uncertainty set, the uncertainty of wind generation forecast is modeled in (3.17) to identify the worst-case solution. $\hat{P}_t^w$ represents the forecasted wind generation. The upper/lower bars in (3.17) represent the upper/lower limits of the uncertainty range, and x is the binary variable to ensure that the upper and lower limits do not occur at the same time (when $\overline{x}$ is one, $\underline{x}$ should be zero and vice versa). Using (3.18), the freedom of binary variables associated with wind generation uncertainty is restricted by the uncertainty limit Γ. The uncertainty limit ensures that the wind generation uncertainty cannot exceed a certain limit, which is bounded by restricting the number of hours during which the uncertain forecast can reach either of its bounds. The robustness of the solution can be further controlled by the uncertainty limit to allow application based on risk-aversion. The risk-aversion solutions are considered as conservative, moderate and aggressive. The conservative solution considers larger

uncertainty limit and provides a more robust solution against uncertainty. Conservative solution results in large total planning cost with lower risk of unserved energy. On other hand, the total planning cost of the aggressive solution (i.e. smaller uncertainty limit) will be small while the solution is less robust than the conservative solution. The moderate solution considers an uncertainty limit between the conservative and aggressive solutions [52].

3.3 Numerical Simulations

The proposed model is applied to IEEE 118-bus test system, as shown in Fig. 3.1, to investigate the model viability. This system has 54 thermal generation units, 186 transmission lines, and 91 loads. A wind farm is considered at bus 2, with a capacity of 200 MW, which has two transmission lines connected to it with maximum capacity of 100 MW each. Table 3.1 shows the characteristics of the BESS to be considered [53], [54]. The proposed planning problem is solved for a one-year period in the following cases:

Case 1: Wind generation curtailment without BESS installation

Case 2: Wind generation curtailment with BESS installation

Case 3: Impact of changing wind farm capacity

Case 4: Considering wind generation uncertainty

Case 5: Impact of changing forecast uncertainty

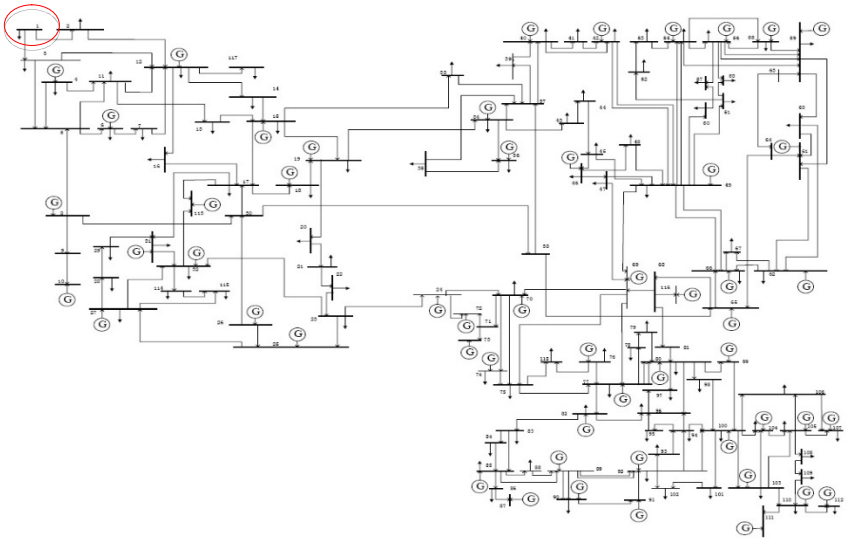

Fig. 3.1 IEEE 118-bus test system

Table 3.1: BESS Characteristics

Power Rating Capital Cost ($/MW-yr)	Energy Rating Capital Cost ($/MWh-yr)	Depth of Discharge (%)	Efficiency (%)
20,000	11,000	80	90

Case 1: In this case, the wind generation is curtailed with no BESS installation. The wind farm has to curtail a total of 4751.7 MWh from its generation, which represents 10.25% of the total wind generation. Fig. 3.2 depicts the total wind generation as well as its curtailment. The total planning cost is found as $234,132,300.

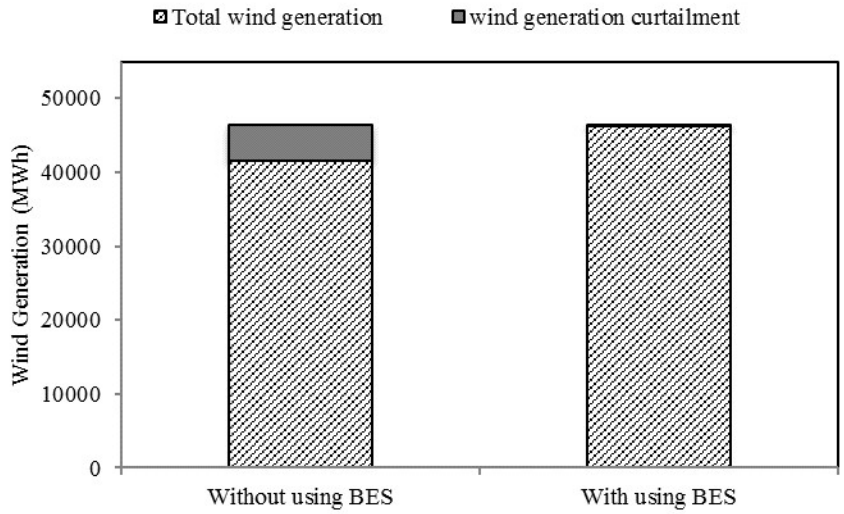

Fig. 3.2 Wind generation versus wind generation curtailment

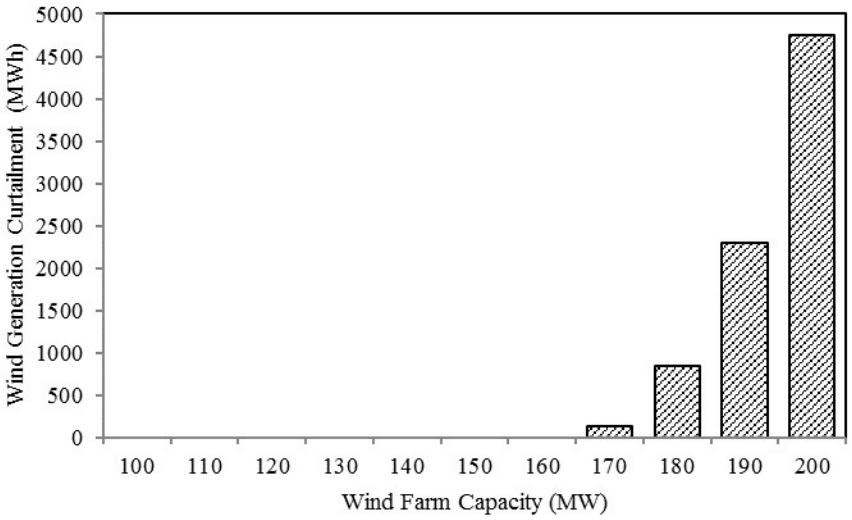

Fig. 3.3 Wind generation curtailment without using BESS

Case 2: In this case, a BESS is considered for installation at the wind farm to investigate the impact of the BESS on the wind generation curtailment. The optimal BESS size is determined to be 32.5 MW and 40.5 MWh for rated power and rated energy, respectively. Using BESS reduces the wind generation curtailment to 36.25 MWh, which represents a reduction of 99% comparing to previous case, as further shown

in Fig 3.2. This is considered a significant reduction of wind generation curtailment as the BESS captures 99% of generation curtailment to use it at other high load demand hours. The total planning cost is decreased in this case to $225,500,500, which is lower than previous case by 3.7%. Table 3.2 summarizes the results from Cases 1 and 2.

Table 3.2: Summary of the Results

	Wind Generation Curtailment (MWh)	Total Operation Cost ($)	Investment Cost ($)	Total System (Planning) Cost ($)
Case 1	4751.7	234,132,300	-	234,132,300
Case 2	36.25	224,405,000	1,095,500	225,500,500
Reduction	99%	4.15%	-	3.7%

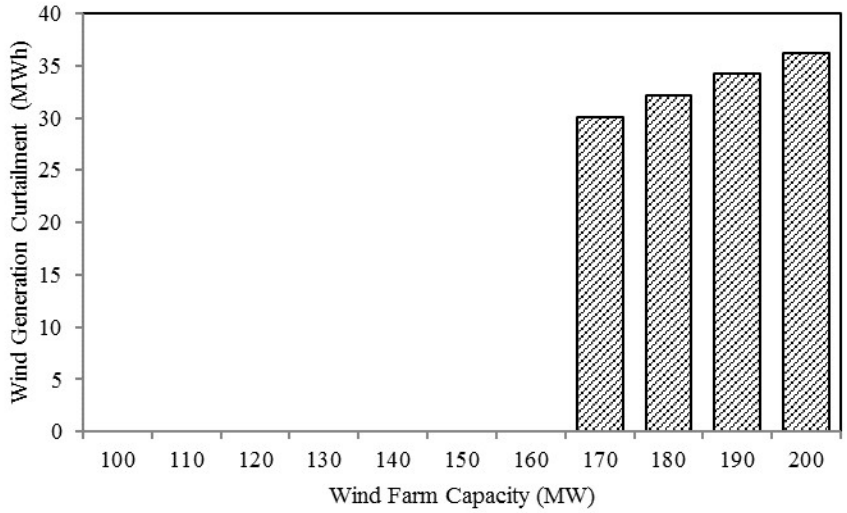

Fig. 3.4 Wind generation curtailment with using BESS

Case 3: In this case, a sensitivity analysis is conducted to investigate the impact of changing the wind farm capacity on wind generation curtailment, the total planning cost, and the optimal BESS size. Figs. 3.3 and 3.4 show the impact of changing wind farm capacity on the wind generation curtailment with and without using BESS. It is found that the wind farm is not required to curtail wind generation when its capacity is

less than or equal to 160 MW. Wind generation starts to be curtailed when the wind farm capacity exceeds 160 MW; however, the curtailed amount of wind generation when using BESS is considerably less than the curtailed amount when BESS is not used (range of 10s of MWhs instead of 1000s of MWhs). In the absence of the BESS, the total planning cost is decreased as wind farm capacity increases, but it starts to increase when the wind generation needs to be curtailed. This is further shown in Fig. 3.5.

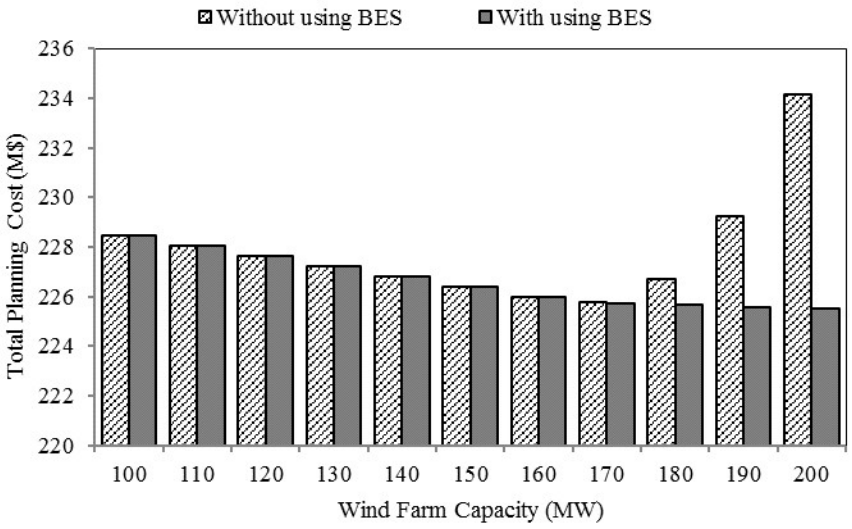

Fig. 3.5 Total planning cost of the power system

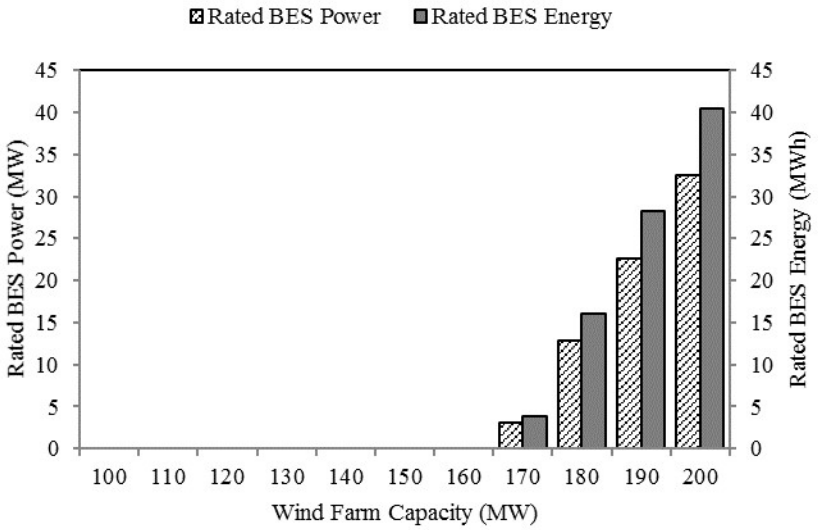

Fig. 3.6 The optimal BESS size versus the wind farm capacity

On the contrary, when using BESS, the total planning cost is decreased when wind farm capacity increases regardless of the required wind generation curtailment, as again shown and compared in Fig. 3.5. Although BESS has a substantial investment cost, the total planning cost keeps decreasing.

Finally, the impact of changing wind farm capacity on the optimal BESS size is investigated. As shown in Fig. 3.6, it is not economical to install BESS when the wind farm capacity is less than or equal 160 MW. Then, the optimal BESS size is increased when the wind farm capacity increases.

Case 4: In this case, the wind generation uncertainty is considered in the robust optimization model to obtain a more practical solution. In this case, the wind generation curtailment is increased to be 43 MWh, i.e., a change of 18.6% compared to case 2. The total planning cost is increased in this case to $225,827,300, which exceeds case 2 by 0.15%. This small increase in the total planning cost increases the solution robustness

against the wind generation uncertainty. Similarly, the optimal BESS size is increased in this case to be 53 MW and 106 MWh for rated power and rated energy, respectively. This is a large increase in BESS size; however, it is required to increase the solution robustness. Figs. 3.7 and 3.8 compare the results in Cases 2 and 4.

Case 5: A sensitivity analysis on changing the upper and lower limits of the uncertainty range is studied to determine the impact of the uncertainty range on the wind generation curtailment and the total system planning cost. The range of uncertainty is selected to be 0, ±5%, ±10%, and ±15%. Fig. 3.9 illustrates the impact of changing the uncertainty range. It is clear that the total planning cost is minimum when there is no forecast uncertainty, which means the forecast is 100% accurate; however, this solution is less practical as this error is almost impossible to achieve. When the uncertainty range increases, the solution robustness against the uncertainty is increased which results in a larger total planning cost. The wind generation curtailment is further increased as the forecast uncertainty increases.

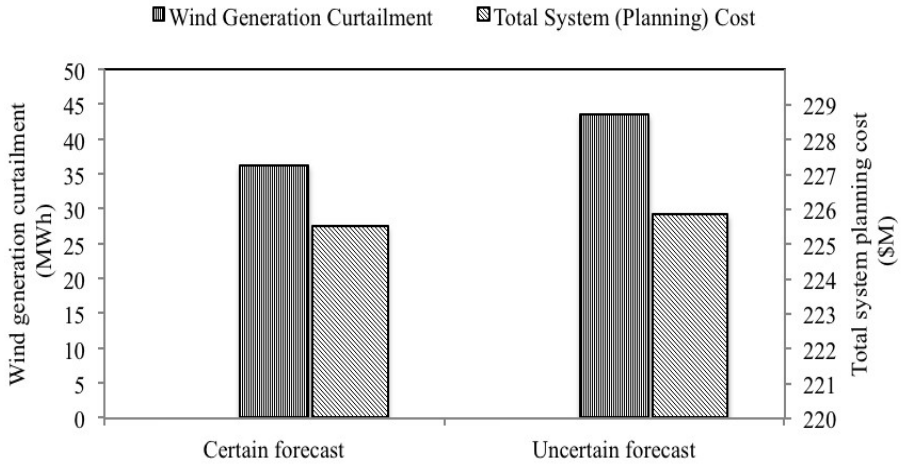

Fig. 3.7 Comparison between Cases 2 and 4 on wind generation curtailment and total planning cost

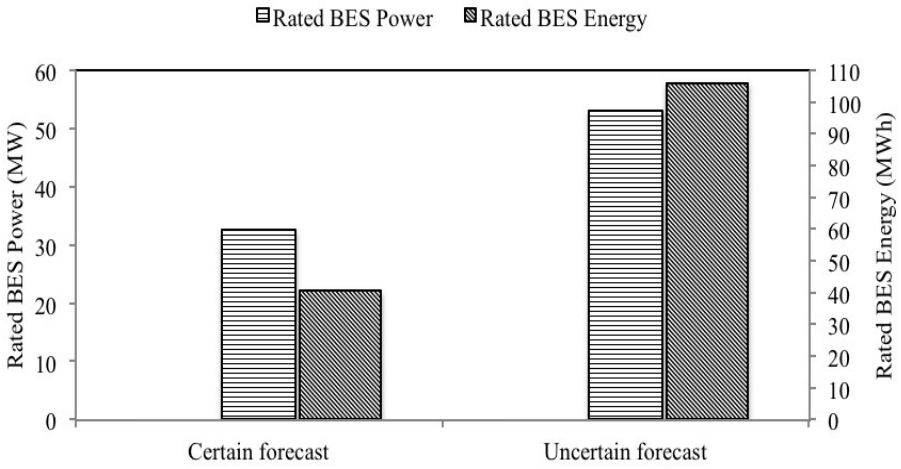

Fig. 3.8 Comparison between Cases 2 and 4 on optimal BESS size

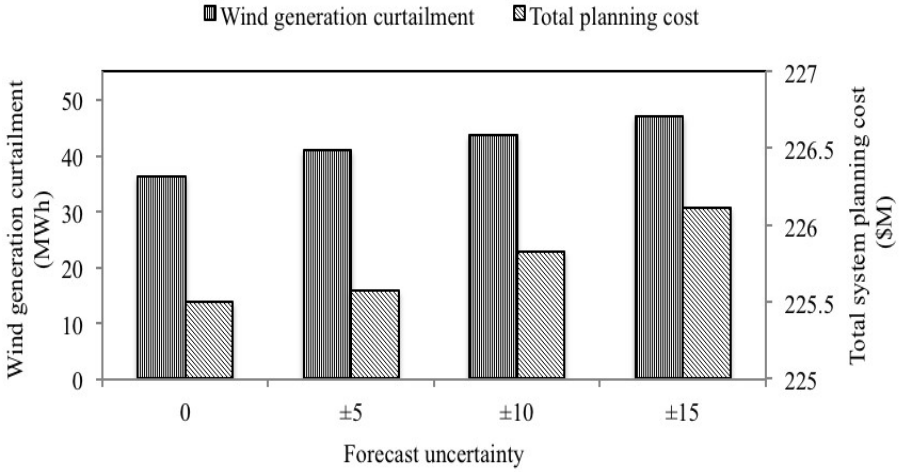

Fig. 3.9 Impact of changing forecast uncertainty

Chapter Four: Managing the Microgrid Net Load Variability

4.1 Introduction

Microgrids are small-scale power systems which consist of at least one distributed energy resource (DER) and one load that are connected to the main distribution grid. The microgrid is an autonomous system; so it can island itself from the utility grid during outage events and reconnect itself when the disturbance is removed. The islanding capability makes the microgrid an important technological development in modern power systems as it can considerably increase the power system resilience and reliability [55]–[58]. Moreover, microgrids facilitate the control and operation of a large number of DERs by utilizing a local controller. Renewable energy resources, such as wind and solar, can also be efficiently integrated to the power system via microgrids.

A reliable coordination of renewable generation within the microgrids requires a viable microgrid scheduling model. The microgrid optimal scheduling problem determines the least-cost schedule of local loads and DERs as well as the transferred power while considering prevailing operational constraints. The microgrid optimal scheduling problem and its formulation can be found in [59]–[62].

This chapter builds upon the available studies in the literature to develop a microgrid optimal scheduling model that incorporates microgrid net load variability limits [63]. This model, furthermore, will be used to analyze the local management option

for limiting microgrid net load variability. The solution will be compared with the central variability management option of installing a centralized power plant from an economic perspective. The levelized cost of energy (LCOE) will be moreover used as an alternative measure to ensure that the decision is made correctly. LCOE is a convenient measure that integrates the capital cost, fuel costs, fixed and variable operations and maintenance (O&M) costs, and financing costs to obtain one fixed number representing the energy cost of any specific generation type [64].

4.2 Model Outline

4.2.1 Microgrid Components

The microgrid components that are modeled in the proposed microgrid optimal scheduling problem include local generation units and loads. The local generation units can be either dispatchable or nondispatchable. Dispatchable units can be controlled by adding operation constraints to the optimal scheduling problem depending on the unit type such as generation limits, minimum on/off time limits, thermal limits, and ramping rate limits. Nondispatchable units are typically renewable energy resources such as wind turbines and solar photovoltaic which cannot be controlled by the microgrid due to the uncontrollable nature of the primary source of energy.

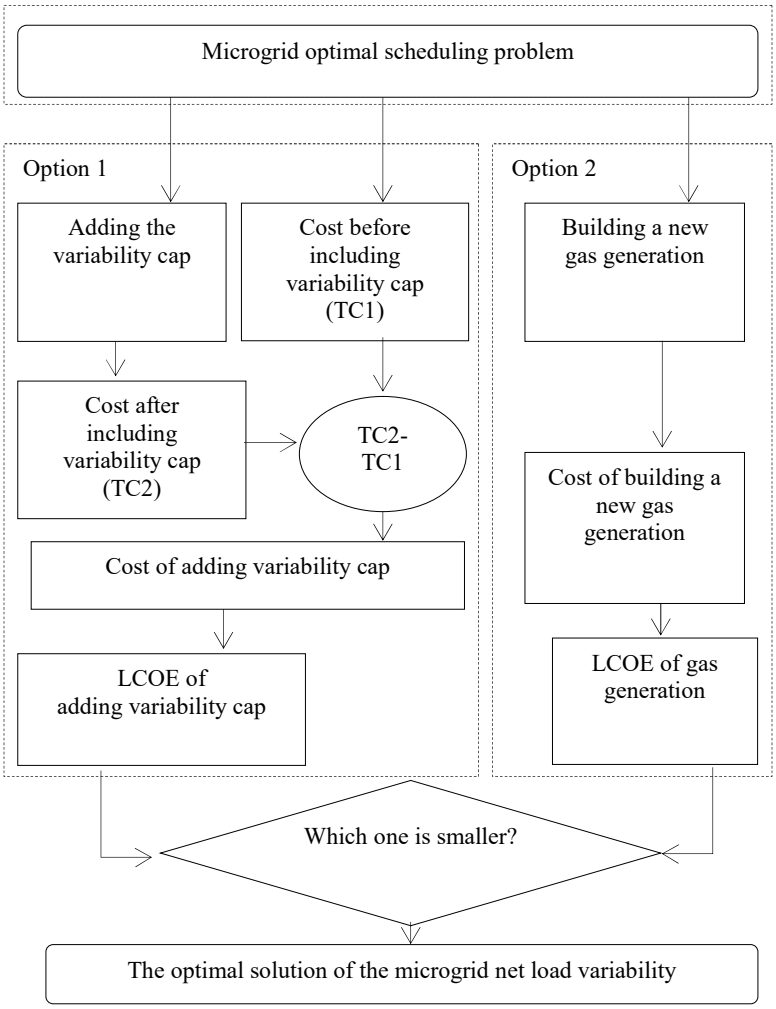

Fig. 4.1 Proposed microgrid net load variability-limiting model

4.2.2 Microgrid net load variability management model

Fig. 4.1 depicts the flowchart of the proposed model. The main objective of this model is to find the optimal solution to limit the microgrid net load variability between two consecutive hours (i.e., a ramping constraint). The model consists of an optimal scheduling problem and two cost calculation problems. The optimal scheduling problem determines the units schedule, the utility transferred power with the microgrid, and the total operation cost of the microgrid before adding the microgrid net load variability constraint. In the local management option, a variability constraint (i.e., a cap) will be

added to the problem to restrict the net load variability between any two consecutive hours. A new utility transferred power flow will be compared with the old one and the impact of adding the constraint is observed. A new total operation cost will be obtained. When the microgrid net load variability is forced to be small between two consecutive hours, the total operation cost will be increased depending. The difference between the new and the old operation costs is calculated to find the cost of adding the cap. In the central management option, a new fast response generation unit (here a gas unit) is considered to be built to deal with the aggregated microgrid net load variability in the distribution level. The planning cost of building the new unit is calculated and annualized. After calculating the cost of both options, a comparison between them will be conducted to find the more economical solution. Alternatively, the LCOE of each option will be calculated in order to enable further comparison. The option that has the smallest LCOE is considered to be the optimal solution of limiting the microgrid net load variability.

4.3 Model Formulation

4.3.1 Microgrid optimal scheduling problem formulation

The microgrid optimal scheduling problem is modeled by mixed-integer programming. The objective of the optimal scheduling problem is to minimize the total operation cost of the microgrid (4.1) subject to operational constraints (4.2)-(4.8). The first term in the objective represents the generation cost of the dispatchable units, no-load cost, and startup and shut down costs. The second term is the cost of purchasing power from the utility grid. The microgrid net load (also known as the transferred utility power)

is the transferred power from or to the microgrid through the point of common coupling (PCC). The transferred power cannot exceed the capacity of the transmission line connecting the utility grid to the microgrid as modeled in (4.2). The microgrid net load might be positive (i.e., microgrid imports power from the utility where the transferred power is less expensive than local generation). On the other hand, when the microgrid net load is negative, microgrid delivers power to the utility grid since the local generation is less expensive than the transferred power. The power balance equation (4.3) guarantees that the summation of local generation and transferred power equals the hourly microgrid net load. The nondispatchable unit generation (here the wind generation) is represented as a negative load in (4.3).

The microgrid components are modeled in (4.4)-(4.8). The maximum and minimum generation capacity limits for each dispatchable unit are modeled by (4.4). The ramping up and down rate limits between two consecutive hours are represented by (4.5)-(4.6). The minimum number of successive hours that the unit can be up or down is shown by (4.7)-(4.8). The commitment state of a dispatchable unit, the startup state and the shutdown state are binary variables. The commitment state *I* will be one when the unit is ON, otherwise it is zero. The startup indicator *y* is one when the unit is started up, otherwise it is zero. The shutdown indicator *z* will be one when the unit is shut down, otherwise it is zero.

$$\min \sum_i \sum_t \sum_d \left[C_i\left(P_{itd}\right) + NL_i I_{itd} + CSU_i y_{itd} + CSD_i z_{itd} \right] + \sum_t \sum_d \rho_{td} P_{M,td} \tag{4.1}$$

$$-P_M^{\max} \le P_{M,td} \le P_M^{\max} \qquad \forall t, \forall d \tag{4.2}$$

$$\sum_i P_{itd} + P_{M,td} = D_{td} - W_{td} \qquad \forall t, \forall d \qquad (4.3)$$

$$P_i^{\min} I_{itd} \le P_{itd} \le P_i^{\max} I_{itd} \qquad \forall i, \forall t, \forall d \qquad (4.4)$$

$$P_{itd} - P_{i(t-1)d} \le RU_i \qquad \forall i, \forall t, \forall d \qquad (4.5)$$

$$P_{i(t-1)d} - P_{itd} \le RD_i \qquad \forall i, \forall t, \forall d \qquad (4.6)$$

$$su_{itd} \ge MU_i z_{i(t+1)d} \qquad \forall i, \forall t, \forall d \qquad (4.7)$$

$$sd_{itd} \ge MD_i y_{i(t+1)d} \qquad \forall i, \forall t, \forall d \qquad (4.8)$$

The startup and shut down indicators are determined as in (4.9)-(4.10). The startup and shut down counters are modeled as in (4.11)-(4.14).

$$I_{itd} - I_{i(t-1)d} = y_{itd} - z_{itd} \qquad \forall i, \forall t, \forall d \qquad (4.9)$$

$$y_{itd} + z_{itd} \le 1 \qquad \forall i, \forall t, \forall d \qquad (4.10)$$

$$0 \le su_{itd} \le MN_i I_{itd} \qquad \forall i, \forall t, \forall d \qquad (4.11)$$

$$\left(MN_i + 1\right) I_{itd} - MN_i \le su_{itd} - su_{i(t-1)d} \le 1 \qquad \forall i, \forall t, \forall d \qquad (4.12)$$

$$0 \le sd_{itd} \le MF_i (1 - I_{itd}) \qquad \forall i, \forall t, \forall d \qquad (4.13)$$

$$1 - \left(MF_i + 1\right) I_{itd} \le sd_{itd} - sd_{i(t-1)d} \le 1 \qquad \forall i, \forall t, \forall d \qquad (4.14)$$

4.3.2 Adding variability cap

The local management option adds a variability cap to the microgrid net load, i.e., the power transferred with the utility grid. The variability cap is modeled in this proposed model for the inter-hour variability (4.15) and the inter-day variability (4.16).

$$\left|P_{M,td} - P_{\mathrm{M},(t-1)d}\right| \le k \qquad \forall t > 1, \forall d \qquad (4.15)$$

$$\left|P_{M,1d} - P_{\mathrm{M},24(d-1)}\right| \le k \qquad \forall t, \forall d > 1 \tag{4.16}$$

The optimal scheduling problem will be used again to find the optimal scheduling of microgrid units after adding the variability limit constraints (4.15) and (4.16). A new microgrid units schedule and a new total operation cost (TC2) will be obtained. The cost of the local management option can be found by calculating the cost increase after adding the variability cap as in (4.17).

$$\text{Option 1: } Cost = TC2 - TC1 \tag{4.17}$$

The variability cap cost ($/yr) will be levelized to obtain the LCOE in $/MWh for the cap value. The LCOE of the variability cap will be compared with the LCOE of gas generation for making the decision on optimal solution.

4.3.3 Building a new gas generation

Building a new gas generation is another option to deal with the increasing variability in the microgrid net load. The cost of building a new gas power generation is divided into capital and operation and maintenance (O&M) costs. The operation cost is also divided into fixed O&M cost and variable O&M cost. The cost of the central management option can be calculated as in (4.18).

$$\text{Option 2: } Cost = \left[\frac{GPC * OCC}{PBP}\right] + \left[GPC * FC\right] + \left[GPC * VC * H\right] \tag{4.18}$$

The LCOE for gas generation is determined in order to compare it with the LCOE for the adding variability cap option.

4.4 Numerical Simulations

The proposed microgrid net load variability-limiting model is applied to a test microgrid with four dispatchable units and one nondispatchable unit (wind turbine). The characteristic of generating units and nondispatchable unit are given in Table 4.1. One-year time horizon of forecasted wind, load and market price is used in the studies. Mixed integer programming is used to model and solve the microgrid optimal scheduling problem. The following cases are studied:

Case 1: Adding a variability cap (local management option)

Case 2: Building a new gas generation (central management option)

Table 4.1: Characteristic of generating units (D: Dispatchable, ND: Nondispatchable)

Unit	Type	Cost Coefficient ($/MWh)	Min.-Max. Capacity (MW)	Min. Up/Down Time (h)	Ramp Up/Down Rate (MW/h)
G1	D	27.7	4-10	3	5
G2	D	39.1	4-10	3	5
G3	D	61.3	2-6	1	3
G4	D	65.6	2-6	1	3
G5	ND	0	0-4.16	-	-

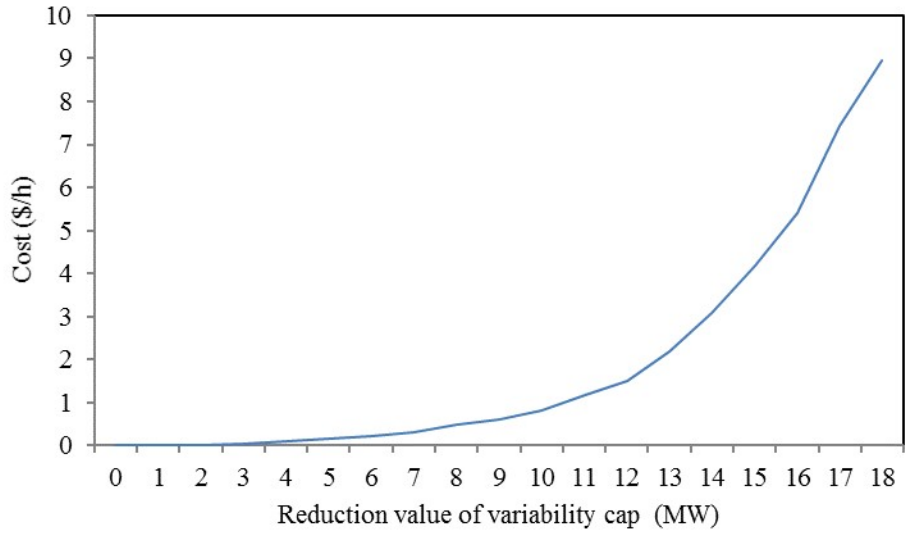

Fig. 4.2 The cost ($/h) of each reduction value of the variability cap

Case 1: Adding a variability cap is the first option to limit the microgrid net load variability. The solved optimal scheduling problem is used as a base case to determine the total operation cost before limiting the microgrid net load variability. Different values of variability cap are added as a constraint to the optimal scheduling problem. The values of variability cap are ranging from 32 to 14 MW, as the maximum power ramp between two consecutive hours is 32 MW. The impact of adding variability cap on the total operation cost is shown in Table 4.2 for each reduction value of the variability cap. Figs. 4.2 and 4.3 show the cost curve and the LCOE curve of each reduction value of the variability cap, respectively.

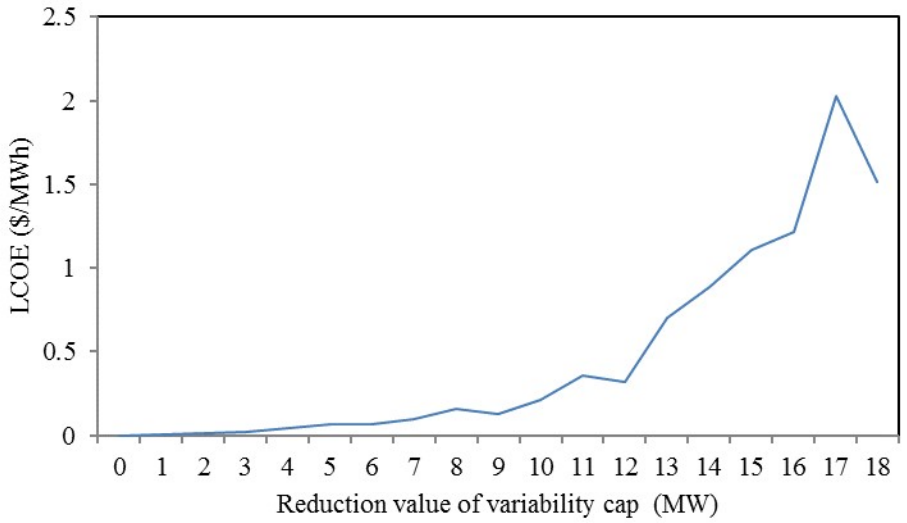

Fig. 4.3 The LCOE ($/MWh) of each reduction value of the variability cap

Table 4.2: The Impact of Adding Variability Cap on the Total Operation Cost

The reduction value of the variability cap (MW)	The Total Operation Cost ($/yr)	Variability Cap Impact ($/yr)	Increased percentage of the total cost (%)
0	3,298,764.81	0.00	0.000
1	3,2988,28.28	63.47	0.002
2	3,298,951.71	186.90	0.006
3	3,299,157.72	392.91	0.012
4	3,299,522.56	757.75	0.023
5	3,300,120.17	1,355.36	0.041

6	3,300,709.51	1,944.70	0.059
7	3,301,531.67	2,766.86	0.084
8	3,302,908.66	4,143.86	0.126
9	3,304,056.97	5,292.16	0.160
10	3,305,888.04	7,123.24	0.216
11	3,309,006.74	10,241.93	0.310
12	3,311,828.03	13,063.22	0.396
13	3,317,997.43	19,232.62	0.583
14	3,325,759.41	26,994.60	0.818
15	3,335,443.35	36,678.54	1.112
16	3,346,110.91	47,346.10	1.435
17	3,363,908.34	65,143.54	1.975
18	3,377,189.12	78,424.31	2.377

Case 2: The second option is building a new gas generation unit in the distribution network to address the microgrid net load variability. The capacity of the gas generation unit should be equal to the variability cap value. The annualized cost of building a 1MW gas generation, which is only for 1 MW/h variability cap, is around $80,000/yr. So, the cost of building a new gas generation is significantly greater than the cost of adding a 1 MW variability cap. Similarly, for the rest of the variability cap values, adding variability cap is more economical than building a new gas generation unit.

Another measure (i.e., the LCOE) is used to decide the more economically viable option. The average LCOE of gas generation in the United States is $66.3/MWh [64]. Fig. 4.4 depicts the LCOE for each variability cap along with the LCOE of gas generation. It is obvious that the gas LCOE is much greater than the LCOE of all variability caps. So, adding a variability cap is always a more viable decision than building a new gas generation unit.

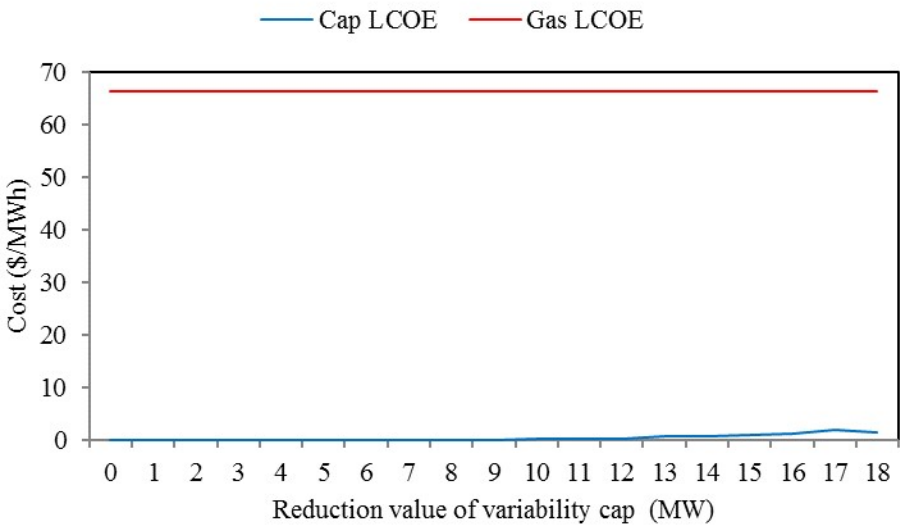

Fig. 4.4 The LCOE of both reduction value of the variability cap and gas generation

Chapter Five: Aggregated Microgrids Net Load Variability in Active Distribution Networks

5.1 Introduction

In this chapter, a security-constrained distribution system market clearing model is proposed. The proactive customers, including microgrids, communicate with the ISO through a DSO. The proposed model considers the system security which consists of distribution lines outages and microgrids' islanding. Following distribution lines outages, microgrids' islanding may happen to avoid load curtailment and protect microgrid loads from upstream disturbances and voltage variations.

5.2 Existing Research on DSOs

The existing work on DSOs focuses on a variety of topics including design, operation, and planning of the DSO, congestion management enabled by the DSO, performance evaluation of this new entity, and grid reliability improvement by the DSO through voltage and reactive power management.

In the context of operation, planning, and economic analysis of the DSO, studies can be found in [37][42][44][65][66][67][68] [69][70][71][72][73][74]. The study in [37] proposes a framework for the day-ahead transactive market which provides an optimal DER scheduling and presents an effective role for the DSO in the power system operation. In the proposed model, the prosumers communicate with the ISO indirectly

through the DSO. In [42], a market-based microgrid optimal scheduling model using DMO is proposed, and a comparison between market-based and price-based microgrid optimal scheduling schemes is provided. It is proved that market-based model outperforms the price-based model in the clearing process of the distribution market by ensuring a lower operation cost and capturing potential uncertainties. In [44], the needs of utilities in managing the challenges of large penetration of proactive customers are addressed by investigating the deployment of a DSO, along with the associated benefits and drawbacks of implementing this concept. In [65], a tariff structure for a large-scale microgrid in the distribution system managed by the DSO is proposed. The model is applied to a real large-scale microgrid which is under construction. The study in [66] presents a neurodynamic price-maker bidding algorithm for the DSO considering power flow constraints and uncertainties of DERs and loads. However, the proposed model is limited in a sense that it can be only applied to balanced distribution systems. The study in [67] proposes a game-based model for long-term multi-period planning of a distribution network composed of several DERs which models the mutual impact of decision making of the DSO on microgrid investment. The objective of the proposed model is to maximize both DSO's and microgrid's profits and reliability during a long-term planning horizon. In [68], a market-based game theory algorithm is proposed to set the customer reliability preferences in smart distribution systems. This model takes into account the interactions among participants and solves the problem using a bilevel optimization approach. The study in [69] presents a long-term dynamic multi-objective model for optimal distribution system planning considering the benefits of the DSO. The

study in [70] introduces a new transactive energy scheme for distribution system planning by demonstrating decentralized energy trading between transactive nodes in transactive coordination systems. In this model, the DSO generates distribution locational marginal prices for transactive nodes. The model considers the uncertainty of load demand, electricity market price, and renewable generation. The study in [71] proposes a number of scenarios for integration of DSOs within the scheduling system. These scenarios are used to investigate the influence of the coordinated market and grid operation approach developed within regenerative renewable electricity system. In [72], a general dual-horizon rolling scheduling model for flexible active distribution system management based on a dynamic AC optimal power flow is proposed. The model provides an optimal operation of distribution system with a high penetration of DERs considering operational uncertainties and market constraints. The study in [73] investigates the future role of the DSO in distribution systems with high penetration of solar PV units. The results show that a certain level of operational real-time interventions by DSOs is inevitable. In [74], a decentralized decision-making method is proposed for optimal power flow implementation between ISOs and DSOs.

Studies in [75][76][77][78][79] focus on DSO-enabled congestion management. In [75], an algorithm to minimize the DSO's operation cost through congestion management using demand-side flexibility is proposed. In [76], the benefits of scheduling flexible residential loads for distribution systems are investigated. The household electricity costs are minimized, and the problem is formulated by bilevel mixed-integer linear programming (MILP). It is shown that harnessing load flexibility allows the DSO

to minimize network congestion. The study in [77] proposes a dynamic management method for congestion management in distribution systems. A coordinative congestion management framework through the coordination of the DSO and a virtual power plant is presented in [78]. This method makes use of flexibility of DERs controlled by a virtual power plant. The study in [79] presents a heuristic optimization model for day-ahead unit commitment in microgrids. This model incorporates a congestion management approach to eliminate congestion by providing an effective unit scheduling according to signals from the DSO.

In the context of DSO performance evaluation, various models are proposed in [80][81][82]. In [80], a framework for performance evaluation of the DSO after a contingency in the system is proposed. Various technical and economic criteria are considered in this process. The optimal size and location of DERs are further determined in this problem. The study in [81] proposes a multi-criteria approach for performance evaluation of DSOs, and discusses that it is important to evaluate DSOs' performance as they face various problems caused by contingencies which should be addressed quickly to maintain power supply quality. The proposed model focuses on five dimensions of the total quality control, where various economic, technical, and personal criteria are used in the problem formulation. The performance of services provided by ISOs and DSOs is investigated in [82] along with a list of new technical regulations' targets to ensure acceptable operation of users connected to the same node in the network.

The DSO's role in reliability improvement is studied in [83][84][85]. The study in [83] emphasizes on the deployment of the DSO to provide the proactive customers with

an efficient and reliable electric power. It is discussed that the DSO is capable of efficiently scheduling DERs to improve system reliability and resiliency on one hand and to reduce emissions and greenhouse gases on the other hand. In [84], a reactive power management model is presented. In the proposed model, the DSO can establish a framework to keep the voltage profile in an acceptable range and reduce the effects of the real power infeed of DGs to the system. A new voltage controller for the DSO that manages an active distribution network is proposed in [85]. The objective of this study is to minimize power losses while obtaining an efficient voltage regulation in the entire system.

The existing work on DSOs as reviewed, particularly on its operation, shows two shortcomings: (1) the importance of contingency scenarios in distribution system management by the DSO is completely overlooked. In other words, it is unclear how the distribution grid will be operated in case of outage of network components or proactive customers, and (2) a focused investigation on the impact of microgrids on the distribution market is not performed. Microgrids show the highest level of flexibility and control among proactive customers [44] and will be core players in distribution markets, so a detailed modeling and analysis of their potential impacts is of great significance.

5.3 Model Outline

This chapter proposes a security-constrained distribution system operation model which maximizes the system social welfare, defined as the load benefit minus the cost of energy purchased from the upstream network. The proposed model is developed for a DSO which is placed between the distribution system and the ISO (Fig. 5.1). Proactive

customers in the distribution grid, including microgrids, send their day-ahead demand bids to the DSO and the DSO sends an aggregated demand bid to the ISO. The ISO runs a day-ahead unit commitment and dispatch, and accordingly sends the awarded power information back to the DSO. The DSO is then responsible for disaggregating and assigning the awarded power to proactive customers based on their original bids. In case of line outages in the distribution system, the operation will not be as straight-forward as in the no-outage case. For example, any microgrid upstream an outaged line can remain connected to the system, while those downstream will switch to the islanded mode, thus completely changing the grid's topology and load profile.

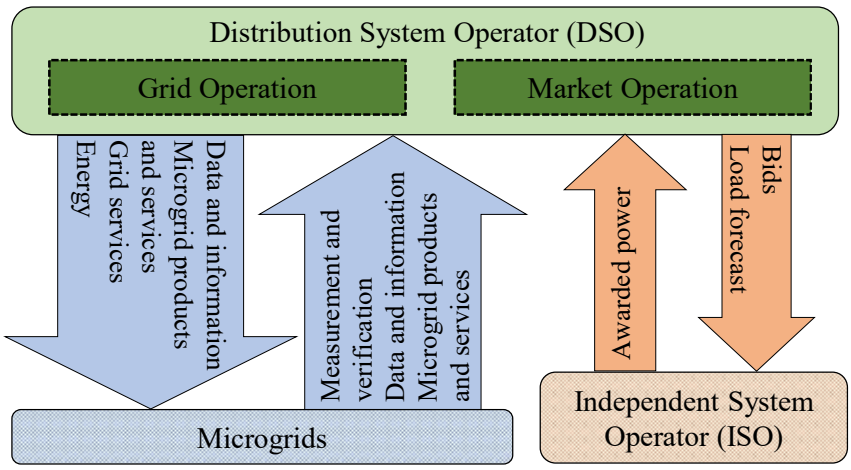

Fig. 5.1. Market structure in the presence of the DSO

The bid sent to the DSO from each microgrid includes the demand curve and the associated ramp rate curve. Fig. 5.2 shows a typical microgrid's demand bid (Fig. 5.2a) and ramp rate curve (Fig. 5.2b). These curves reveal the following information to the DSO: 1) the microgrid fixed load which is not curtailable and should be fully supplied in both normal and contingency cases; 2) different price bids of the exchanged power that

microgrid can import from the DSO (when in the positive side of the demand bid curve) or export to the DSO (when in the negative side of the demand bid curve); and 3) the ramp rate of each load segment; for example, when the exchanged power between the microgrid i and the DSO occurs in load segment 1, the ramp rate of this segment should be RRi1.

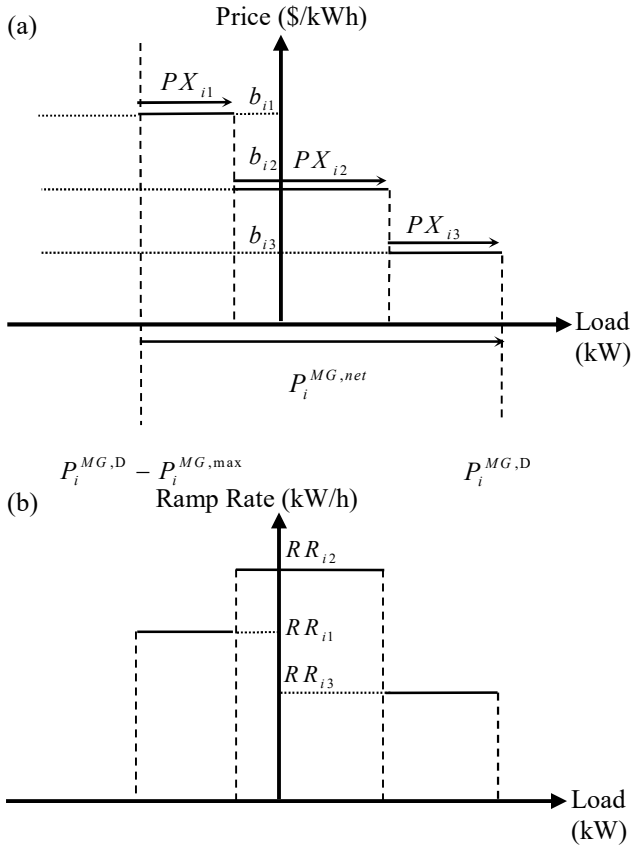

Fig. 5.2 Microgrid's (a) demand bid and (b) ramp rate curve

The proposed security-constrained distribution system operation model is developed based on a set of linear AC power flow equations, thus is capable of solving a full AC power flow and accordingly identifying the impact of real and reactive power injections, as well as thermal overload and voltage magnitudes. The proposed model further considers an N-1 security criterion, which simply means that the system can

adequately supply the loads in case of single component outages at any given time. A reliability cost is further considered to account for potential power outages in contingency cases.

The proposed model is capable of modeling microgrid islanding in case of upstream disturbances. In other words, if the status of a line changes from operational to outage, any microgrid upstream that line can remain connected to the grid, while those downstream would be islanded and must supply their loads locally. Fig. 5.3 shows an illustrative example in which the system is initially in the normal operation (Fig. 5.3a). If line 1 is on outage, the fixed load (which is outside the microgrids) will not be supplied and both microgrids A and B become islanded (Fig. 5.3b). If line 2 is on outage, the fixed load will be supplied from the main grid, while both microgrids A and B become islanded (Fig. 5.3c) as the fixed load is upstream the outaged line, but both microgrids are downstream. If line 3 is on outage, only microgrid B switches to the islanded mode while the fixed load is supplied and microgrid A remains connected to the grid (Fig. 5.3d). In all cases that microgrids are islanded, they would supply their loads locally.

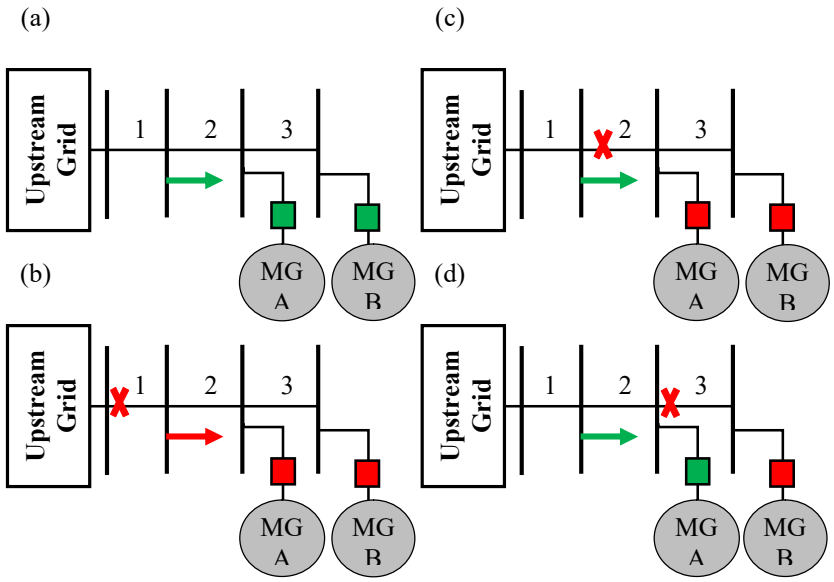

Fig. 5.3. Microgrid islanding in case of power disturbance in the upstream lines

5.4 Model Formulation

The distribution system social welfare is defined as load benefit minus the system cost, which comprises the cost of purchasing energy from the upstream grid plus the cost of unserved energy in case of system outages (5.1). The load benefit is the dollar amount that microgrids are willing to pay for a desired level of supplied power. The exchanged energy with the upstream grid can be positive, when imported, or negative, when exported to the upstream grid. The cost of unserved energy represents the reliability cost and is defined as the value of lost load (VOLL) times the hourly amount of scenario-based load curtailment. The VOLL depends on various factors and represents customers' willingness to pay in order to avoid power interruptions [86]. The cost of unserved reactive power is defined as a small positive constant times the amount of reactive power not supplied. There is no actual cost for reactive power curtailment, however this term is added to ensure solution feasibility in case of lack of adequate reactive power in the grid.

This small cost coefficient ensures that this term is relatively smaller than other terms in the objective and thus does not impact the solution optimality.

Index s represents contingency scenarios in which $s=0$ is associated with the normal operation mode and $s\geq 1$ are associated with contingency scenarios.

$$\max\left(\sum_{i\in \mathrm{D_m}}\sum_{t} B_i(P_{it0}^{\mathrm{MG,net}}) - \sum_{c\in \mathrm{C_m}}\sum_{t}\lambda_{ct}^{\mathrm{T}}P_{ct0}^{\mathrm{M}} - \sum_{m}\sum_{t}\sum_{s}\vartheta^{P}PS_{mts} - \sum_{m}\sum_{t}\sum_{s}\vartheta^{Q}QS_{mts}\right) \quad (5.1)$$

The objective function (5.1) is subject to nodal load balance constraints (5.2)-(5.6), network power flow constraints (5.7)-(5.13) and microgrid constraints (5.14)-(5.21).

Nodal load balance:

$$\sum_{c\in \mathrm{C_m}} P_{cts}^{\mathrm{M}} + \sum_{n\in \mathrm{B_m}} PL_{mnts} = \sum_{i\in \mathrm{D_m}} P_{its}^{\mathrm{MG,net}} + PD_{mt} - PS_{mts} \qquad \forall m,\forall t,\forall s \quad (5.2)$$

$$\sum_{c\in \mathrm{C_m}} Q_{cts}^{\mathrm{M}} + \sum_{n\in \mathrm{B_m}} QL_{mnts} = \sum_{i\in \mathrm{D_m}} Q_{its}^{\mathrm{MG,net}} + QD_{mt} - QS_{mts} \qquad \forall m,\forall t,\forall s \quad (5.3)$$

$$-P_{c}^{\mathrm{M,max}} \leq P_{cts}^{\mathrm{M}} \leq P_{c}^{\mathrm{M,max}} \qquad \forall c,\forall t,\forall s \quad (5.4)$$

$$0 \leq PS_{mts} \leq PD_{mt} \qquad \forall m,\forall t,\forall s \quad (5.5)$$

$$0 \leq QS_{mts} \leq QD_{mt} \qquad \forall m,\forall t,\forall s \quad (5.6)$$

Network power flow:

$$\begin{aligned} &M(1-w_{mnts}) \leq PL_{mnts} - g_{mn}(\Delta V_{mts} - \Delta V_{nts}) + b_{mn}(\Delta\theta_{mts} - \Delta\theta_{nts}) \\ &-g_{mn}\Delta\hat{V}_{mts}(\Delta V_{mts} - \Delta V_{nts}) \leq M(1-w_{mnts}) \qquad \forall mn\in \mathrm{L},\forall t,\forall s \end{aligned} \quad (5.7)$$

$$\begin{aligned} &M(1-w_{mnts}) \leq QL_{mnts} + b_{mn}(\Delta V_{mts} - \Delta V_{nts}) + g_{mn}(\Delta\theta_{mts} - \Delta\theta_{nts}) \\ &+b_{mn}\Delta\hat{V}_{mts}(\Delta V_{mts} - \Delta V_{nts}) \leq M(1-w_{mnts}) \qquad \forall mn\in \mathrm{L},\forall t,\forall s \end{aligned} \quad (5.8)$$

$$-PL_{mn}^{\max} w_{mnts} \leq PL_{mnts} \leq PL_{mn}^{\max} w_{mnts} \qquad \forall mn\in \mathrm{L},\forall t,\forall s \quad (5.9)$$

$$-QL_{mn}^{\max} w_{mnts} \le QL_{mnts} \le QL_{mn}^{\max} w_{mnts} \qquad \forall mn \in \mathrm{L}, \forall t, \forall s \qquad (5.10)$$

$$\Delta\theta_{1ts} = 0 \qquad \forall t, \forall s \qquad (5.11)$$

$$\Delta V_{1ts} = 0 \qquad \forall t, \forall s \qquad (5.12)$$

$$\Delta V_m^{\min} \le \Delta V_{mts} \le \Delta V_m^{\max} \qquad \forall m, \forall t, \forall s \qquad (5.13)$$

Microgrid constraints:

$$\left(P_{it}^{\mathrm{MG,D}} - P_i^{\mathrm{MG,max}}\right) I_{its} \le P_{its}^{\mathrm{MG,net}} \le P_{it}^{\mathrm{MG,D}} I_{its} \qquad \forall i, \forall t, \forall s \qquad (5.14)$$

$$\left(Q_{it}^{\mathrm{MG,D}} - Q_i^{\mathrm{MG,max}}\right) I_{its} \le Q_{its}^{\mathrm{MG,net}} \le Q_{it}^{\mathrm{MG,D}} I_{its} \qquad \forall i, \forall t, \forall s \qquad (5.15)$$

$$P_{its}^{\mathrm{MG,net}} = P_{its}^{\mathrm{MG,D}} - \sum_j PX_{ijts} \qquad \forall i, \forall t, \forall s \qquad (5.16)$$

$$\varepsilon \le I_{its} + \sum_{nm \in \mathrm{L}_i} a_{mni} - \sum_{nm \in \mathrm{L}_i} a_{mni} w_{mnts} \le 1 \qquad \forall i, \forall t, \forall s \qquad (5.17)$$

$$\left| P_{its}^{\mathrm{MG,net}} - P_{i(t-1)s}^{\mathrm{MG,net}} \right| \le RR_{its}^{\mathrm{sel}} \qquad \forall i, \forall t, \forall s \qquad (5.18)$$

$$0 \le PX_{ijts} \le \delta_{ijts} PX_{ij}^{\max} \qquad \forall i, \forall j, \forall t, \forall s \qquad (5.19)$$

$$\sum_j \delta_{ijts} = 1 \qquad \forall i, \forall t, \forall s \qquad (5.20)$$

$$-M(1-\delta_{ijts}) \le RR_{its}^{\mathrm{sel}} - RR_{ij} \le M(1-\delta_{ijts}) \qquad \forall i, \forall j, \forall t, \forall s \qquad (5.21)$$

The nodal load balance equations for real and reactive power are represented by (5.2) and (5.3), respectively. These equations ensure that the net real and reactive power supplied through the network to each bus equal the net load of that bus. Real and reactive load curtailment variables are further added to these equations to ensure feasibility in case of supply shortage. Each microgrid's exchanged power with the utility grid can be

positive (when the microgrid imports power) or negative (when the microgrid exports power). As presented in (5.2) and (5.3), when a microgrid imports power from the grid, it is considered as a demand by the DSO, while treated as a generation source when exporting power. The amount of real power supplied by the upstream grid cannot exceed the capacity of the line connecting the upstream grid to the distribution grid (5.4). Furthermore, the real and reactive hourly load curtailments at each bus are limited by the associated hourly real and reactive load demands as shown in (5.5) and (5.6).

The nonlinear AC power flow equations are linearized following the method proposed in [87], [88]. Linear power flow equations for real and reactive powers are represented by (5.7)-(5.10). These equations consider line outage by defining parameter w which is 0 when the line is out of service and 1 when it is operational. If the line is out of service, (5.7) and (5.8) would be relaxed and (5.9) and (5.10) set the real and reactive power flows in that line to zero. On the other hand, when the line is in service, (5.7) and (5.8) would force the line flow equation and (5.9) and (5.10) dictate the line limit. It should be noted that the term $\Delta\hat{V}_{mts}$ (ΔV_{mts} - ΔV_{nts}) in (5.7)-(5.8) is nonlinear and solved in two steps. In the first step, the term $\Delta\hat{V}_{mts}$ (ΔV_{mts} - ΔV_{nts}) is considered zero to obtain a linear model. Once solved, the calculated $\Delta\hat{V}_{mts}$ is plugged back to the equations to solve the model again. Detailed discussions of this two-step method can be found in [87] and [88].

Variables ΔV_m and $\Delta\theta_m$ are the variations in voltage magnitude and angle for each bus relative to that of POI. The POI is considered as a reference bus with voltage magnitude of 1 pu and an angle of 0 degrees. These variations are zero at the reference

bus (5.11)-(5.12). To ensure there will be no voltage violation in downstream distribution buses, (5.13) is imposed.

Constraints (5.14) and (5.15) constrain microgrids' exchanged real and reactive powers between their minimum and maximum limits, further considering microgrids' islanding state. At each time, the minimum would be the microgrid load minus the microgrid's maximum local generation capacity, and the maximum would be the microgrid fixed load (i.e., in case of no local generation). The binary microgrid islanding variable I_{its} is set to 0 when the microgrid operates in the islanded mode and to 1 when it operates in the grid-connected mode. This variable is multiplied by the limits in (5.14) and (5.15) to force the microgrid net power to zero in case of islanding. The exchanged power of each microgrid is equal to the microgrid fixed load minus the sum of all selected demand segments (5.16). Equation (5.17) determines microgrid islanding based on the state of the upstream lines in the distribution system. If all upstream lines are operational, the microgrid remains connected to the grid, otherwise becomes islanded. Ramp rate constraints are represented by (5.18)-(5.21). The changes of power exchange of all microgrids in two consecutive hours cannot exceed the selected ramp rate (5.18). A binary variable δ is considered for each segment which is set to 1 when that segment is selected, and set to 0 otherwise. The microgrids' demand segments are limited by their minimum and maximum power (5.19). Equation (5.20) ensures that only one segment is selected for each microgrid. The selected ramp rate of each microgrid at any given time is determined by (5.21). If a segment is selected (associated with δ=1), the selected ramp rate would be equal to that segment's ramp rate.

5.5 Numerical Simulations

The proposed model is applied to a modified IEEE 33-bus test system as shown in Fig. 5.4. This system has 33 buses, 32 distribution lines, and 11 fixed loads. A total of 4 microgrids is considered in this system, with respective POIs as shown. Of the 32 distribution lines, 17 lines considered to be within these microgrids. The distribution system is connected to the upstream grid via bus 1. The microgrids' characteristics are summarized in Table 5.1. The hourly electricity market price and the microgrids' hourly fixed load data are listed in Tables 5.2 and 5.3, respectively. Three price segments are assumed for each microgrid's bid. Microgrids' ramp rate is assumed to be 50% of their respective capacity in each segment. VOLL is considered as $10/kWh [89]. The problem is formulated as mixed integer linear programming (MILP) and solved by CPLEX 12.6 [90]. Following cases are discussed:

Case 0: Normal system operation without contingency scenarios

Case 1: Security-constrained operation considering N-1 contingency without microgrids' islanding

Case 2: Security-constrained operation considering N-1 contingency with microgrids' islanding

Case 3: Security-constrained operation considering only the outage of the line connected to the distribution network POI

Case 4: Impact of microgrids' islanding on nodal prices

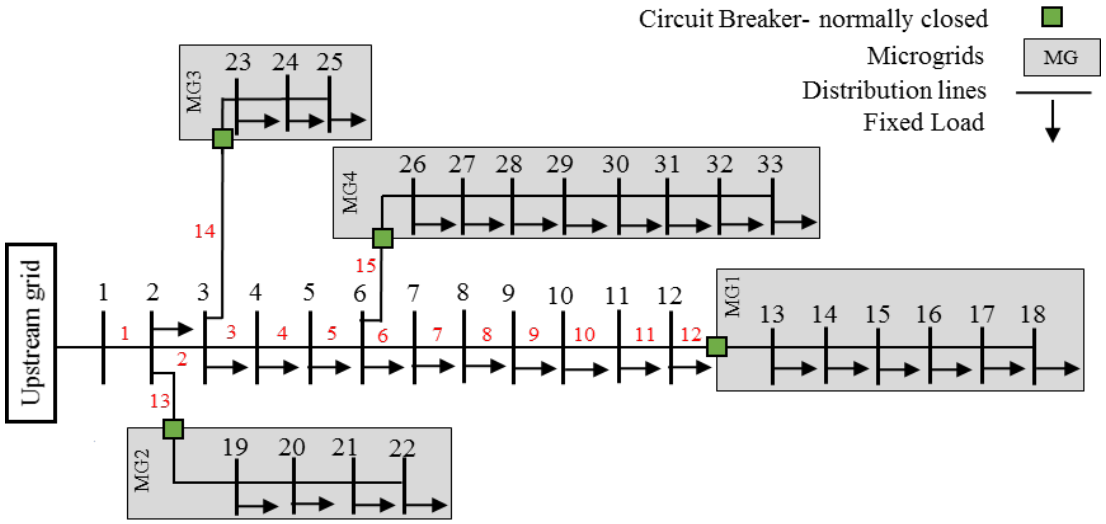

Fig. 5.4. Modified IEEE 33-bus standard test system

Table 5.1: Microgrids' Characteristics

	MG 1	**MG 2**	**MG 3**	**MG 4**
	Price ($/kWh)			
Segment 1	0.065	0.072	0.085	0.089
Segment 2	0.039	0.064	0.065	0.069
Segment 3	0.017	0.019	0.025	0.029
	Ramp Rate (kW/h)			
Segment 1	50	35	50	75
Segment 2	50	40	100	125
Segment 3	100	75	200	150
	Capacity (kW)			
Segment 1	100	70	100	150
Segment 2	100	80	200	250
Segment 3	200	150	400	300

Table 5.2: Electricity Price ($/kWh)

Hour	1	2	3	4	5	6	7	8
Price	0.015	0.011	0.0135	0.0154	0.0185	0.0218	0.0173	0.0228
Hour	9	10	11	12	13	14	15	16
Price	0.0218	0.0271	0.0371	0.069	0.0658	0.0666	0.0654	0.0798
Hour	17	18	19	20	21	22	23	24
Price	0.1155	0.1103	0.0961	0.0905	0.0774	0.071	0.0594	0.0567

Table 5.3: Microgrids' Fixed Load (kW)

MG 1								
Hour	1	2	3	4	5	6	7	8
Load	318	316	315	315	315	315	333	326
Hour	9	10	11	12	13	14	15	16
Load	325	326	330	330	331	330	330	330
Hour	17	18	19	20	21	22	23	24
Load	331	324	318	316	316	316	315	313
MG 2								

Hour	1	2	3	4	5	6	7	8
Load	254	253	252	252	252	252	266	260
Hour	9	10	11	12	13	14	15	16
Load	259	260	263	263	264	263	263	263
Hour	17	18	19	20	21	22	23	24
Load	264	258	254	253	253	253	252	250
MG 3								
Hour	1	2	3	4	5	6	7	8
Load	656	653	651	651	651	651	688	673
Hour	9	10	11	12	13	14	15	16
Load	671	673	681	681	683	681	681	681
Hour	17	18	19	20	21	22	23	24
Load	683	668	656	653	653	653	651	646
MG 4								
Hour	1	2	3	4	5	6	7	8
Load	649	646	644	644	644	644	681	666
Hour	9	10	11	12	13	14	15	16
Load	664	666	674	674	676	674	674	674
Hour	17	18	19	20	21	22	23	24
Load	676	661	649	646	646	646	644	639

Case 0: In this case, normal distribution system operation without contingency scenarios (line outages) is studied. The optimal operation problem is solved for one day, i.e., 24 h, in which the total load benefit, the cost of purchased energy from upstream grid and the reliability cost are calculated as \$1424, \$1429 and \$0, respectively. There is no load curtailment as no outage is considered in this case. The exchanged power of all microgrids with the upstream grid is shown in Fig. 5.5. The exchanged powers change over hours due to the changes in the electricity price. When the electricity price is high, the imported power decreases, while when the price is low, the microgrids switch to local generation and even in some cases sell excess generation back to the grid (associated with negative exchanged power). It should be noted that microgrids 3 and 4 have higher fixed load compared to that of microgrids 1 and 2, thus their respective exchanged power is relatively higher. Furthermore, the energy from the upstream grid is less expensive than microgrids' local generation in early hours of the day, thus all microgrids would import

power from the upstream grid to supply their loads. However, due to the high price of the upstream grid's energy during peak hours, the microgrids prefer to locally supply their loads and sell the excess power back to the grid. No outage is considered in this case, so microgrids are scheduled to achieve the highest social welfare possible without concerns for reliability. To increase the system reliability, it is important to consider the system contingency when solving the optimal operation problem which is investigated in following cases.

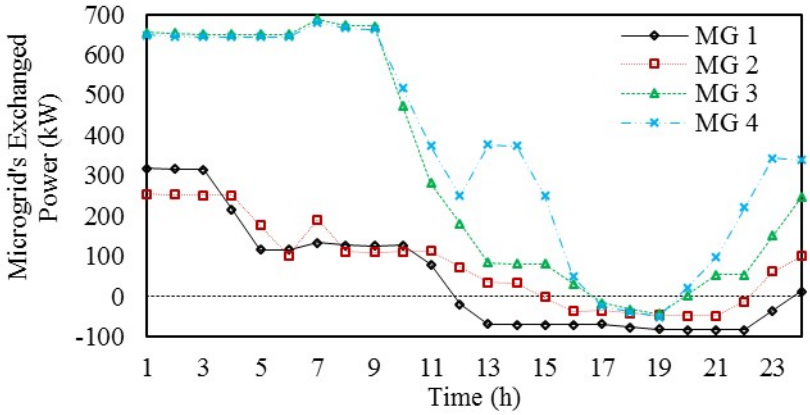

Fig. 5.5. Microgrids' exchanged power in Case 0, without contingency scenarios

Case 1: In this case, system contingency is considered while assuming microgrids would not switch to an islanded mode, regardless of the upstream lines' contingencies. In other words, microgrids are treated as prosumers that own and operate local DERs but do not have an islanding capability. An N-1 contingency is considered, which includes the outages of all 15 lines in 24 hours (a total of 360 scenarios). The total load benefit and cost of upstream purchased energy are calculated as \$905 and \$1134, respectively. Following line outages, the load benefit and the cost of upstream purchased energy are decreased because microgrids' exchanged power is reduced as shown in Fig. 5.6.

Moreover, loads are partially curtailed due to line outages. Fig. 5.7 shows the average load curtailment at each bus. The total average load curtailment in this case is calculated as 206.2 kWh. As shown in Fig. 5.7, the load curtailments occur both inside and outside of microgrids. The average load curtailment in microgrids' buses is 151.8 kWh, whereas it is 54.4 kWh on buses outside microgrids. This case shows that the microgrids' loads would be curtailed when microgrids do not have the islanding capability. The load curtailment in microgrids is undesirable as the purpose of microgrids deployment is to improve system reliability by avoiding load curtailments. Therefore, it is extremely important to consider microgrids' islanding in case of system contingencies.

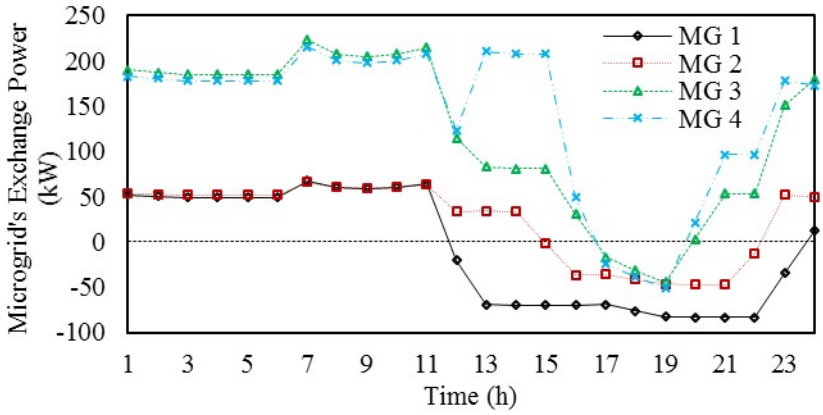

Fig. 5.6. Microgrids' exchanged power with the upstream grid for Cases 1

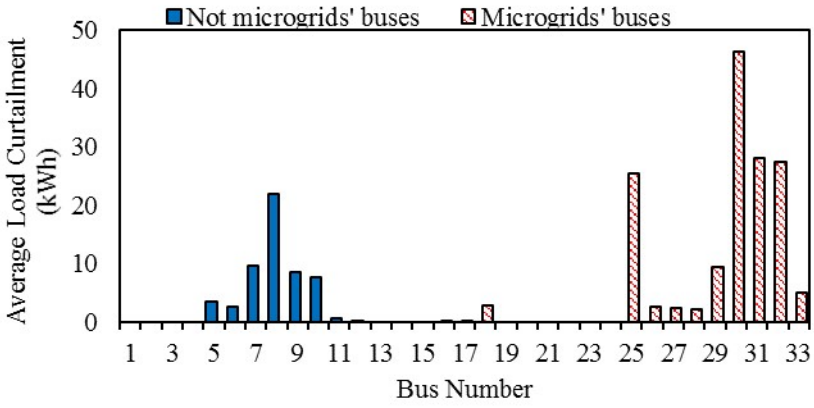

Fig. 5.7. Average load curtailment for all scenarios in Case 1

Case 2: In this case, similar contingency scenarios as in Case 1 are considered while considering microgrids islanding. The total benefit and cost of upstream purchased energy are respectively calculated as $1053 and $1198, which show an increase of 16.4% and 5.5%, respectively, compared to the previous case. Moreover, the total benefit is decreased by 26% compared to Case 0 (base case). This loss of benefit is considered as the expense of obtaining a more practical solution by considering line contingencies. Fig. 5.8 illustrates the exchanged power of all microgrids when simultaneously considering contingency scenarios and microgrids' islanding. The exchanged power in this case still has a somewhat similar profile to that of previous cases, especially in terms of power import/export. However, the imported power from the upstream grid is generally decreased compared to Case 0 mostly over early hours of the day. The reason of this decrease in power import is that line outages result in microgrid islanding, therefore microgrids turn on local generation resources to ensure adequate reserve capacity for switching to the islanded mode whenever needed. However, the microgrids' exchanged power is increased compared to Case 1, and that explains the 16.4% increase of the total load benefit in this case. This increase in the exchanged power happens due to islanding capability in which microgrids can island during power outages to protect their loads from curtailment. The total average load curtailment in this case is calculated as 281.9 kWh. Fig. 5.9 shows the average load curtailment at each bus in this case. As shown in Fig. 5.9, all load curtailments occur on buses outside microgrids as there is no curtailment of microgrids loads. This result shows that the microgrid reliability is improved compared to Case 1. It is worth mentioning that the average load curtailment is increased

by 36.7% compared to Case 1, but all load curtailments in this case are outside microgrids. In other words, these loads are only supplied by the upstream grid in case of microgrids' islanding. As a result, the load curtailments are inevitable in case of contingency that causes power interruption at upstream grid. The computation time in this case is about one hour.

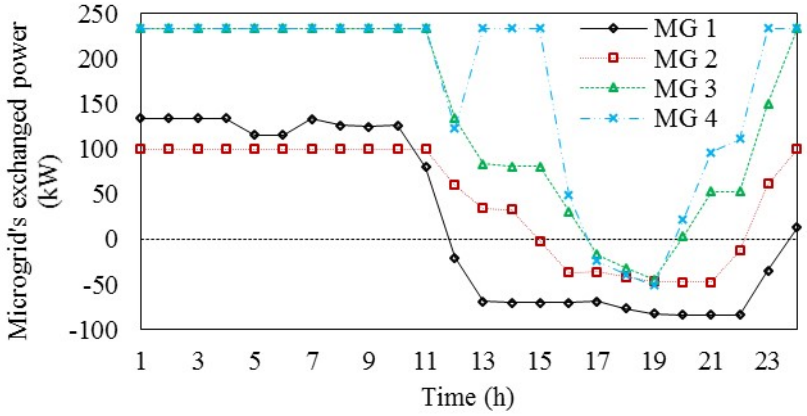

Fig. 5.8. Microgrids' exchanged power with the upstream grid for Cases 2

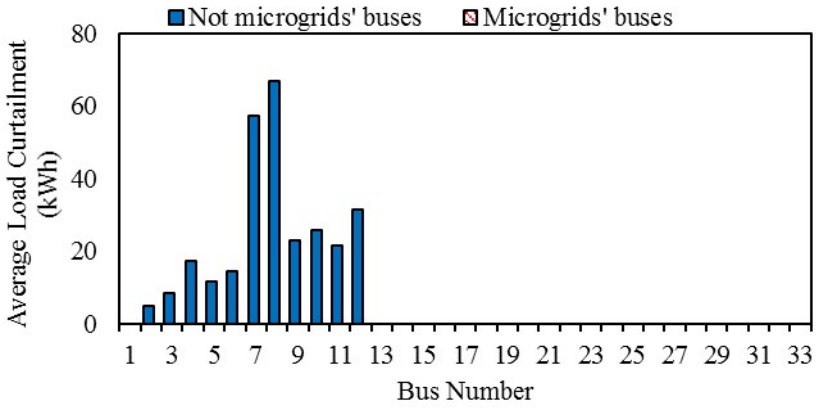

Fig. 5.9. Average load curtailment for all scenarios in Case 2

Case 3: The contingency of only the first line connecting the distribution system to the upstream grid in 24 hours (a total of 24 scenarios) is studied in this case. This case is selected because the outage of line 1 represents the worst-case scenario. The results in this case are very close to those of Case 2. Therefore, this case can be used for

simulations instead of Case 2 with much less computation time which is about 2 minutes. The total benefit is calculated as $1051 which is very close to the result of Case 2 (0.19% difference). This small error is negligible as the exchanged power of all microgrids is also very close to the results of exchanged power in Case 2.

Case 4: The nodal prices of the buses outside microgrids when a microgrid switches to the islanded mode are studied in this case. The nodal prices are calculated in Case 0 under normal operation (i.e., no line outages and all microgrids operate in the grid-connected mode). In this case, only microgrid 1 is selected to be islanded in two scenarios: when the microgrid is importing power (hour 1) and the when it is exporting power (hour 20). The nodal prices after islanding are compared to those in Case 0 as shown in Figs. 5.10 and 5.11. When the microgrid imports power, it acts as a load in the distribution system, therefore when islanded, the total load in the system would decrease. As a result, the nodal prices would decrease (Fig. 5.10). However, when the microgrid exports power to the upstream grid, it acts as a generator. If the microgrid switches to the islanded mode, the total generation in the system would decrease. Hence, the nodal prices would increase (Fig. 5.11). This case clearly shows the impact that the microgrid islanding can make on nodal prices of the network, and accordingly, on market clearing and settlement. It further highlights the important role of islanding considerations in distribution markets.

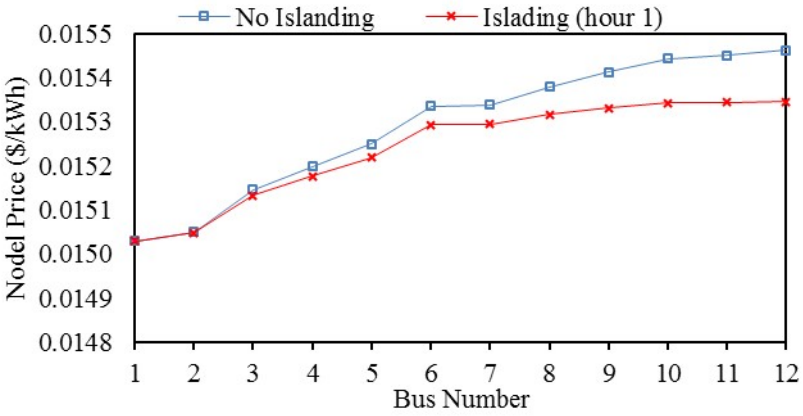

Fig. 5.10. Nodal prices under microgrid 1 islanding during power import

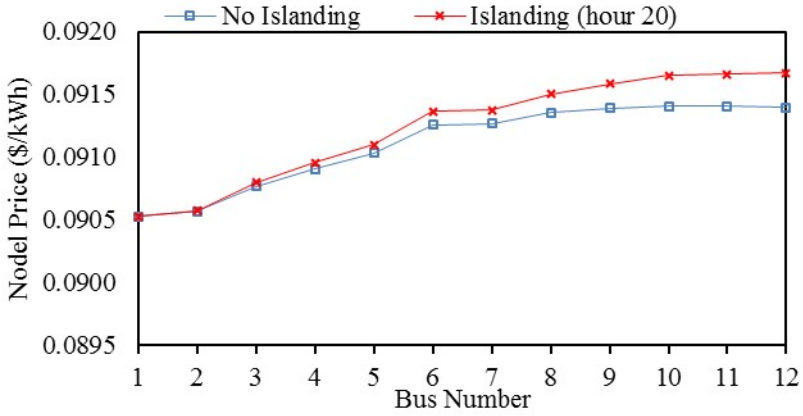

Fig. 5.11. Nodal prices under microgrid 1 islanding during power export

5.6 Discussions

The proposed model aims at modeling and analyzing the impacts of microgrid participation in the distribution market. According to the studied cases, the following could be concluded:

- The system social welfare decreases when considering contingency scenarios. The reason of this decrease is that the microgrids' generation cost is increased due to the increase of their power generation to overcome the power delivery interruption which is caused by contingencies. In this case, microgrids would have less exchanged power, and they should supply their loads with their local generation. As a result,

microgrids' participation in the distribution market would be lower, hence a lower benefit. However, microgrids' reliability increases in response to lines contingencies when islanding is considered.

- Without considering microgrids' islanding capability (treating microgrids as prosumers), there would be load curtailment in microgrids in case of line contingency in the upstream grid. The reason is the loads downstream the contingency would be curtailed and the local generation of nearby microgrids would supply those loads outside their boundaries. As a result, the microgrids become overloaded and cannot fully supply their local loads. However, considering islanding capability would improve microgrids reliability by making them operate in islanded mode and supplying their local loads only.
- In all cases, the exchanged power does not significantly change in early hours of the day, but it changes during the peak hours. The reason is that in early hours, the upstream grid's energy is less expensive than local generation, therefore microgrids import as much power as possible from the upstream grid to supply local loads. In other words, the exchanged power follows microgrids' fixed load profile. However, during peak hours, the upstream grid's energy becomes more expensive than local generation, hence the microgrids' local generation would increase to minimize their operation cost. As a result, the exchanged power follows the extra generation in microgrids.
- The contingency scenarios of only the first line connecting the distribution system to the upstream grid is the worst-case scenario where the results in this case are almost

the same as in the case considering all line contingency scenarios. Solving the proposed model with considering only the first line's contingency helps significantly reduce the computation time by decreasing the number of scenarios.

- If a microgrid switches from the grid-connected to the islanded mode, the network nodal prices will accordingly change. This change depends on the microgrid power exchange status, in which in case of power import, the nodal prices would drop and in case of power export the nodal prices would go up.

Chapter Six: Impact of Grid Reconfiguration in Distribution Market Clearing and Settlement

6.1 Introduction

In this chapter, a distribution market clearing model is proposed to maximize the local social welfare while supporting grid reliability. This least-cost reliability-constrained objective is achieved through grid reconfiguration, i.e., a grid topology control. This chapter builds on the existing work in this area and focuses on maximizing the social welfare in the distribution market through grid reconfiguration.

6.2 Model Outline and Formulation

The proposed model aims at reconfiguring the distribution grid using the smart switches in order to maximize the system social welfare. The system social welfare is defined as the load benefit minus the cost of purchasing energy from the upstream grid (6.1).

$$\max\left(\sum_{i\in \mathrm{D_m}} B_i(P_i^{MG}) - \sum_{c\in \mathrm{C_m}} \lambda_c^T P_c^M\right) \tag{6.1}$$

where, i is the index for number of flexible loads, and or microgrids, in the distribution system and c is the index for the points of interconnection (POI) with the upstream grid. $B(.)$ represents the load benefit of flexible loads, i.e., the amount that customers are willing to pay for a desired level of power. λ^T and P^M represent the price and amount of power exchange with the upstream grid, respectively. The objective function is subject to

operational and radiality constraints. Active and reactive power balance constraints are represented in (6.2) and (6.3), respectively, to ensure the supply-demand balance for all buses.

$$\sum_{c\in \mathrm{C_m}} P_c^M + \sum_{n\in \mathrm{B_m}} PL_{mn} + \sum_{i\in \mathrm{D_m}} P_i^{MG} = PD_m \qquad \forall m \tag{6.2}$$

$$\sum_{c\in \mathrm{C_m}} Q_c^M + \sum_{n\in \mathrm{B_m}} QL_{mn} + \sum_{i\in \mathrm{D_m}} Q_i^{MG} = QD_m \qquad \forall m \tag{6.3}$$

where, PL_{mn} and QL_{mn} represent the distribution line active and reactive power flow from bus m to bus n. P^{MG} and Q^{MG} are the flexible load active and reactive power, and PD_m and QD_m represent the fixed load active and reactive power. The line that connects the distribution grid to the upstream grid has a capacity limit as represented in (6.4). Similarly, the flexible loads need to be within certain operation limits as represented in (6.5) and (6.6).

$$-P_c^{M,\max} \le P_c^M \le P_c^{M,\max} \qquad \forall c \in \mathrm{C_m} \tag{6.4}$$

$$P_i^{MG,\min} \le P_i^{MG} \le P_i^{MG,\max} \qquad \forall i \in \mathrm{D_m} \tag{6.5}$$

$$Q_i^{MG,\min} \le Q_i^{MG} \le Q_i^{MG,\max} \qquad \forall i \in \mathrm{D_m} \tag{6.6}$$

The proposed model is developed using a linearized AC power flow. The details of linearization can be found in [88]. Active and reactive AC power flow equations are represented in (6.7) and (6.8), respectively. The distribution lines' capacity is modeled by (6.9) and (6.10) to impose active and reactive power flow limits.

$$-M(1-w_{mn}) \le PL_{mn} - g_{mn}(\Delta V_m - \Delta V_n) + b_{mn}(\Delta\theta_m - \Delta\theta_n) - g_{mn}\Delta V_m(\Delta V_m - \Delta V_n) \le M(1-w_{mn}) \quad \forall mn \in \mathrm{L} \tag{6.7}$$

$$-M(1-w_{mn}) \le QL_{mn} + b_{mn}(\Delta V_m - \Delta V_n) + g_{mn}(\Delta\theta_m - \Delta\theta_n) + b_{mn}\Delta V_m(\Delta V_m - \Delta V_n) \le M(1-w_{mn}) \quad \forall mn \in \mathrm{L} \tag{6.8}$$

$$-PL_{mn}^{\max} w_{mn} \le PL_{mn} \le PL_{mn}^{\max} w_{mn} \qquad \forall mn \in \mathrm{L} \tag{6.9}$$

$$-QL_{mn}^{\max} w_{mn} \le QL_{mn} \le QL_{mn}^{\max} w_{mn} \qquad \forall mn \in \mathrm{L} \tag{6.10}$$

where, M is a large positive number which is used to relax the power flow equations when the line is switched off, and w_{mn} is a state variable which is used to decide the state of distribution lines (w_{mn} is 1 when the switch is closed and 0 otherwise). When the state variable of the distribution line, i.e., w_{mn}, is 0, (6.9) and (6.10) force to switch off the line and make sure no power flows in that line, whereas (6.7) and (6.8) would be relaxed. On the other hand, the distribution line would be in service when w_{mn} = 1. Thus, the power flow limits (6.9) and (6.10) allow the power flow in the line and (6.7) and (6.8) would be forced. ΔV_m and $\Delta\theta_m$ are the variations in voltage magnitude and angle for each bus relative to the POI. The POI bus is considered as a reference bus with voltage magnitude of 1 pu and an angle of 0 degrees. These variations are constrained by (6.11) to make sure there will be no voltage violation in the distribution buses.

$$\Delta V_m^{\min} \le \Delta V_m \le \Delta V_m^{\max} \qquad \forall m \tag{6.11}$$

The radial structure of the distribution grid should not be affected by the grid reconfiguration. The term “radial structure” means that all nodes are connected but they do not form any loops. The radiality constraint (6.12) is added to make sure the distribution system stays radial and does not form loops.

$$\sum_{mn \in \Gamma} w_{mn} \le L - 1 \qquad \forall mn \in \mathrm{L} \tag{6.12}$$

where, L is the number of distribution lines in each possible loop. This constraint would force the number of closed lines to be one less than the number of lines that can form a loop. Hence, there should be one open line in each potential loop.

6.3 Numerical Simulations

The proposed model is tested on a modified IEEE 33-bus distribution system shown in Fig. 6.1. This system consists of 33 buses, 32 sectionalizing switches (normally close), 5 tie switches (normally open), 29 fixed loads, and 3 microgrids. Closing any tie switch would form a loop. All potential loops are shown in Table 6.1. The proposed formulation is modeled by mixed integer linear programming (MILP) and solved using CPLEX 12.6. It is solved for only one-hour; however, it can be extended to be solved for any other selected time horizon, including day-ahead. The total fixed load is 2620 kW, and the generation capacity of each microgrid is 1000 kW. The market price at the POI is \$0.070/kWh. The fixed load of microgrids 1, 2, and 3 at this selected hour are 63.379 kW, 296.204 kW, and 42.427 kW, respectively. Table 6.2 shows the microgrids characteristics. The proposed model is solved for two cases with and without grid reconfiguration to show the impact on the results.

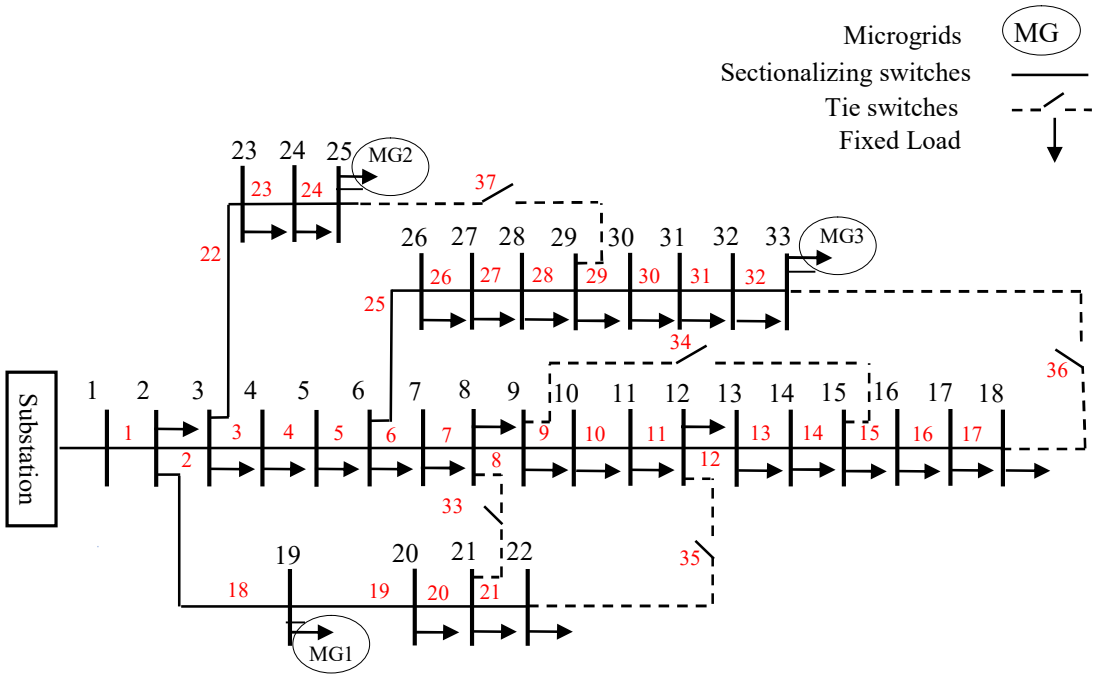

Fig. 6.1. The IEEE 33-bus distribution test system

Table 6.1: The potential loops

Loop No.	Lines in the loop
1	2, 3, 4, 5, 6, 7, 18, 19, 20, 21, 33
2	9, 10, 11, 12, 13, 14, 34
3	2, 3, 4, 5, 6, 7, 8, 9, 10, 11, 18, 19, 20, 21, 35
4	6, 7, 8, 9, 10, 11, 12, 13, 14, 15, 16, 17, 25, 26, 27, 28, 29, 30, 31, 32, 36
5	3, 4, 5, 22, 23, 24, 25, 26, 27, 28, 37

Table 6.2: Microgrids' Characteristics

Segments	1		2		3	
	Quantity (kW)	Price ($/kW)	Quantity (kW)	Price ($/kW)	Quantity (kW)	Price ($/kW)
Microgrid 1	500	0.065	300	0.039	200	0.027
Microgrid 2	450	0.072	350	0.065	200	0.029
Microgrid 3	400	0.085	400	0.064	200	0.035

Case 1: Without grid reconfiguration: In this case, the proposed model is solved for a one-hour period without allowing any changes in the grid topology. This is achieved by forcing all tie switches to stay open by fixing the state variable w_{mn}=0. The social welfare is calculated as $150.54. The total power purchase from the upstream grid is 1233.09 kW. Microgrids 1, 2, and 3 generate 703.949 kW, 600 kW, and 142.418 kW,

respectively. The total power loss is calculated as 59.46 kW. In this case, the payment to the upstream grid is $86.32, and the customers' payment to the DSO is $183.88.

Case 2: With grid reconfiguration: In this case, the grid reconfiguration is considered in the proposed model. This is accomplished by allowing the state variables of the tie and sectionalizing switches to change (to either 0 or 1) in the optimization problem. In this case the optimal grid reconfiguration is achieved by closing 2 tie switches (36 and 37) and simultaneously opening 2 sectionalizing switches (15 and 22) to prevent forming loops in the distribution system. The social welfare is increased in this case to $153.56, which is more than the previous case by 2%. The total power purchase from the upstream grid is 616.76 kW, which is decreased by 49.98% compared to previous case. In this case microgrids 1, 2, and 3 generation are increased by 7.1%, 66.67%, and 104.16%, respectively. The total power loss is decreased by 30.26% compared to the previous case, reaching 41.47 kW. Moreover, the payment to the upstream grid in this case is $43.17, which is decreased by 49.98%. However, the customers' payment to the DSO is increased by 1.02% to $185.76. The upstream grid payment is decreased as the power purchase from the upstream grid is dropped, and instead power is purchased locally from microgrids to maximize the system social welfare. As a result, microgrids generation is increased in in this case compared to Case 1. Table 6.3 and Fig 6.2 compare the market clearing and power flow results in Cases 1 and 2, respectively.

Table 6.3: Comparison between results of Cases 1 and 2

		Without Reconfiguration	With Reconfiguration	Change
Social Welfare ($)		150.54	153.56	2%
Upstream power purchase (kW)		1233.09	616.76	-49.98%
Microgrids power (kW)	MG1	703.949	753.949	7.1%
	MG2	600	1000	66.67%
	MG3	142.418	290.765	104.16%
Power Loss (kW)		59.46	41.47	-30.26%
Upstream grid payment ($)		86.32	43.17	-49.98%
Customers payment ($)		183.88	185.76	1.02%

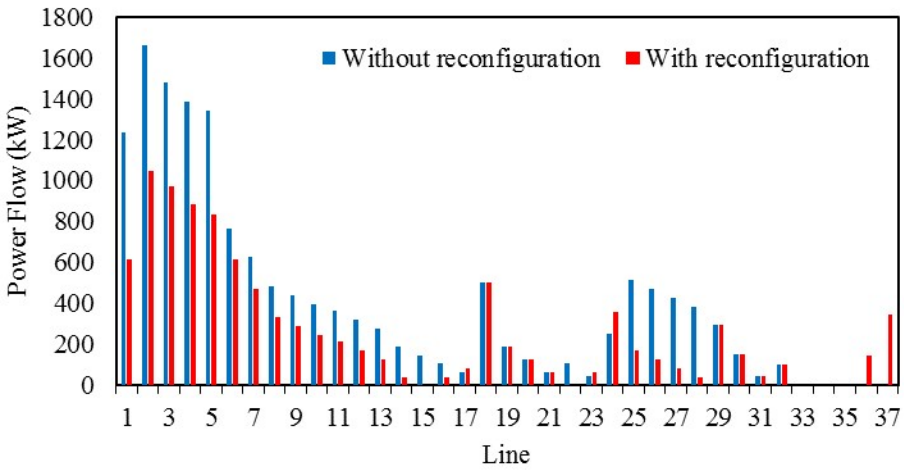

Fig. 6.2. Power flow comparison between cases 1 and 2

As shown in Fig 6.2, the power flow when reconfiguration is not considered is high for most of the lines compared to the case with reconfiguration. This is because of the opportunity that is provided for local generators, within microgrids, to supply local loads and change the grid power flow. This change in power flow also helps reduce the power loss as shown in the results.

Chapter Seven: Conclusion and Future Work

7.1 Conclusion

This dissertation investigated the challenge of generation variability resulted from renewable energy resources integration in both transmission and distribution levels in modern power systems. Two subtopics were covered by this dissertation to overcome variability challenges of renewable energy resources integration. The first was variability of renewable energy resources on transmission level. The second was variability of microgrid net load on distribution level through microgrid-integrated renewable generation and based on a DSO-operated energy market.

In chapter two, a hybrid model for smoothing wind power fluctuations was proposed and tested and analyzed on a large-scale wind farm. Two methods were considered to work simultaneously, were the first method investigated dumping of generated wind power to smooth the wind power considering a certain limit, and the second method investigated the application of the BESS for the same purpose. The proposed hybrid model was examined on three cases: without BESS, with fixed BESS capacity, and with optimal BESS capacity. The wind power profile was less variable in all cases, but the smoothing quality was different in each case. The wind farm profit in all three cases was further calculated for comparison purposes. The results illustrated that using the proposed hybrid model on the wind farm could identify the most economical

solution for addressing the wind power variability. Since the power curtailment is an energy waste and it is not desirable, chapter three proposed a planning model to reduce wind generation curtailment. The model was capable of determining the optimal amount of wind generation curtailment based on transmission network congestion while at the same time finding the optimal BESS size, thus it could efficiently minimize the energy waste caused by wind generation curtailment. Simultaneously, the proposed model was capable of determining the worst-case solution under prevailing uncertainty of wind generation forecast. The proposed model was tested on the standard IEEE 118-bus test system with a wind farm and a BESS. Five cases were examined by using the proposed model where the comparison of the results showed the effectiveness of the proposed model. The numerical simulations further exhibited that using BESS technology is valuable as both the total planning cost and the wind generation curtailment were remarkably reduced. Numerical simulations, furthermore, investigated how the wind farm capacity affected the decision of installing BESS as well as curtailing the wind generation. Moreover, it investigated the considering of the wind generation uncertainty in the planning problem. The total planning cost, wind generation curtailment and the optimal BESS size, however, were increased compared to ignoring uncertainty. As a result, including wind forecast uncertainty provided a more practical solution to avoid further investments in support of existing electricity infrastructure.

An efficient model for limiting the microgrid net load variability was proposed in chapter four. Two options were considered, were the first option investigated the addition of a variability cap to limit the microgrid net load variability within two successive hours

and the second option investigated the addition of a new gas generation unit to the distribution system. The impact of adding the cap on the total operation cost in the first option was noticed by comparing the microgrid total operation cost in both cases (i.e., the original solution and the solution after adding the variability cap). The difference was considered to be the cost of adding variability cap. The cost of build a new gas generation and the LCOE of gas generation were further calculated for comparison purposes. The model was tested and analyzed on a microgrid test system. The numerical simulations were shown that adding a variability cap on the microgrid net load was always the more economical solution for addressing the microgrid net load variability. The aggregated microgrids net load variability was investigated in this dissertation when the microgrids penetration increased in distribution level. This was accomplished by considering DSO to clear the distribution market. Two models were proposed in chapters five and six. Chapter five proposed a security-constrained distribution system operation model to maximize the system social welfare by increasing microgrid participation in the distribution market. The model was applied to a modified IEEE 33-bus standard test system, and contingency scenarios were defined as outage of one line at each hour (N-1 criteria). The proposed model was capable of modeling microgrid islanding based on contingencies in the upstream lines. The results showed that the microgrids changed their operation in response to contingency scenarios compared to the normal operation, and as a result, the total benefit decreased. The results further showed the importance of considering microgrids' islanding capability in improving microgrid's reliability. When considering microgrids' islanding capability, load curtailment in microgrids was avoided.

Therefore, it was concluded that it would be crucial to simultaneously consider contingency and microgrids' islanding capability in distribution market clearing. It was also shown that the contingency scenario of the first line in the distribution system could be used instead of considering all line outages as the results were almost the same. However, the computation time significantly reduced because only 24 scenarios were considered. Finally, chapter six proposed a grid reconfiguration model to maximize the social welfare in a distribution market. The proposed model was also tested on a modified IEEE 33-bus distribution system. The results showed that the social welfare could be improved by applying the grid reconfiguration. Moreover, the proposed model showed the capability to serve as a congestion relief and loss reduction method by revising the power flow within the grid. Overall, the proposed model advocated that the reconfiguration can provide a level of flexibility in distribution markets to improve the system social welfare and help with better utilization of distributed resources within radial distribution grids.

7.2 Future Work

The DSO model in this dissertation focuses only on energy market without considering other distribution system ancillary services. Therefore, the DSO role in the distribution systems can be extended to consider and clear different ancillary services markets. Ancillary services that could be consider in the DSO model include regulation and reserve markets. In addition, the impact of electric vehicles (EVs) presence in the distribution system could be investigated in terms of distribution market clearing.

References

[1] J. Smith and B. Parsons, “Wind Integration [Guest Editorial],” *IEEE Power Energy Mag.*, vol. 9, no. 6, pp. 18–25, Nov. 2011.

[2] M. H. Albadi and E. F. El-Saadany, “The role of taxation policy and incentives in wind-based distributed generation projects viability: Ontario SOP case study,” in *Power Symposium, 2008. NAPS’08. 40th North American*, 2008, pp. 1–6.

[3] “European Renewable Energy Council (EREC).” [Online]. Available: http://www.erec.org/fileadmin/erec_docs/Documents/Publications/Renewable_Energy_Technology_Roadmap.pdf.

[4] W. A. Omran, M. Kazerani, and M. M. A. Salama, “Investigation of Methods for Reduction of Power Fluctuations Generated From Large Grid-Connected Photovoltaic Systems,” *IEEE Trans. Energy Convers.*, vol. 26, no. 1, pp. 318–327, Mar. 2011.

[5] J. Charles Smith and Brian Parsons, “Wind Integration Much Has Changed In Two Years,” *IEEE Power Energy Mag.*, 2011.

[6] C. Nayar, “Remote area micro-grid system using diesel driven doubly fed induction generators, photovoltaics and wind generators,” in *Sustainable Energy Technologies, 2008. ICSET 2008. IEEE International Conference on*, 2008, pp. 1081–1086.

[7] A. Keane *et al.*, “Capacity Value of Wind Power,” *IEEE Trans. Power Syst.*, vol. 26, no. 2, pp. 564–572, May 2011.

[8] E. Denny and M. O'Malley, "Quantifying the Total Net Benefits of Grid Integrated Wind," *IEEE Trans. Power Syst.*, vol. 22, no. 2, pp. 605–615, May 2007.

[9] "GLOBAL WIND REPORT 2016 | GWEC." [Online]. Available: http://www.gwec.net/publications/global-wind-report-2/global-wind-report-2016/. [Accessed: 23-Jun-2017].

[10] "GLOBAL WINDSTATISTICS 2017 | GWEC." [Online]. Available: http://gwec.net/wp-content/uploads/vip/GWEC_PRstats2017_EN-003_FINAL.pdf. [Accessed: 20-Mar-2018].

[11] J. E. S. de Haan, J. Frunt, and W. L. Kling, "Mitigation of Wind power Fluctuation in Smart Grids," 2010, pp. 1–8.

[12] P. Sorensen *et al.*, "Power Fluctuations From Large Wind Farms," *IEEE Trans. Power Syst.*, vol. 22, no. 3, pp. 958–965, Aug. 2007.

[13] H. H. Zeineldin, T. H. M. El-Fouly, E. F. El-Saadany, and M. M. A. Salama, "Impact of wind farm integration on electricity market prices," *IET Renew. Power Gener.*, vol. 3, no. 1, p. 84, 2009.

[14] L. Bird, J. Cochran, and X. Wang, "Wind and solar energy curtailment: experience and practices in the United States," *NREL March*, 2014.

[15] M. Pucci and M. Cirrincione, "Neural MPPT Control of Wind Generators With Induction Machines Without Speed Sensors," *IEEE Trans. Ind. Electron.*, vol. 58, no. 1, pp. 37–47, Jan. 2011.

[16] "State Energy Conservation office." [Online]. Available: http://www.seco.cpa.state.tx.us/re_wind-incentives.htm. [Accessed: 08-Jul-2017].

[17] P. Poonpun and W. T. Jewell, “Analysis of the Cost per Kilowatt Hour to Store Electricity,” *IEEE Trans. Energy Convers.*, vol. 23, no. 2, pp. 529–534, Jun. 2008.

[18] C. Wu, H. Mohsenian-Rad, J. Huang, and A. Y. Wang, “Demand side management for wind power integration in microgrid using dynamic potential game theory,” in *GLOBECOM Workshops (GC Wkshps), 2011 IEEE*, 2011, pp. 1199–1204.

[19] “FlexibleResourcesHelpRenewables_FastFacts.pdf.” [Online]. Available: http://www.caiso.com/Documents/FlexibleResourcesHelpRenewables_FastFacts.pdf. [Accessed: 08-Jul-2017].

[20] D. Hayashi, T. Senjyu, R. Sakamoto, N. Urasaki, T. Funabashi, and H. Sekine, “Generating power leveling of renewable energy for small power system in isolated island,” in *Intelligent Systems Application to Power Systems, 2005. Proceedings of the 13th International Conference on*, 2005, pp. 6–pp.

[21] J. E. S. de Haan, J. Frunt, A. Kechroud, and W. L. Kling, “Supplementary Control for Wind Power Smoothing,” in *Universities Power Engineering Conference (UPEC), 2010 45th International*, Cardiff, Wales, 2010, pp. 1–5.

[22] A. Esmaili and A. Nasiri, “Power smoothing and power ramp control for wind energy using energy storage,” in *2011 IEEE Energy Conversion Congress and Exposition*, Phoenix, AZ, 2011, pp. 922–927.

[23] M. Jannati, S. H. Hosseinian, B. Vahidi, and G. Li, “A significant reduction in the costs of battery energy storage systems by use of smart parking lots in the power fluctuation smoothing process of the wind farms,” *Renew. Energy*, vol. 87, pp. 1–14, Mar. 2016.

[24] V. Akhmatov and P. Bø. Eriksen, “A Large Wind Power System in Almost Island Operation—A Danish Case Study,” *IEEE Trans. Power Syst.*, vol. 22, no. 3, pp. 937–943, Aug. 2007.

[25] Yuan-Kang Wu, Ching-Yin Lee, and Ging-He Shu, “Taiwan’s First Large-Scale Offshore Wind Farm Connection—A Real Project Case Study With a Comparison of Wind Turbine,” *IEEE Trans. Ind. Appl.*, vol. 47, no. 3, pp. 1461–1469, May 2011.

[26] C. Klumpner, B. Al, and D. Hann, “A power electronic controlled dump load with negligible harmonics for accurate loading used in testing small wind turbines,” in *Industrial Electronics (ISIE), 2010 IEEE International Symposium on*, 2010, pp. 596–601.

[27] S. V. Papaefthymiou, E. G. Karamanou, S. A. Papathanassiou, and M. P. Papadopoulos, “A Wind-Hydro-Pumped Storage Station Leading to High RES Penetration in the Autonomous Island System of Ikaria,” *IEEE Trans. Sustain. Energy*, vol. 1, no. 3, pp. 163–172, Oct. 2010.

[28] D. Lew *et al.*, “Wind and solar curtailment,” in *International Workshop on Large-Scale Integration of Wind Power Into Power Systems*, 2013.

[29] S. Fink, C. Mudd, K. Porter, and B. Morgenstern, “Wind energy curtailment case studies,” *NREL Oct.*, 2009.

[30] J. Rogers, S. Fink, and K. Porter, “Examples of wind energy curtailment practices,” *Exeter Assoc. Inc Subcontract Rep. No NRELSR-550-48737*, 2010.

[31] “Renewable curtailment: one symptom of grid troubles.” [Online]. Available: http://blog.enbala.com/renewable-curtailment. [Accessed: 27-Jul-2017].

[32] “CAISO: California curtailed 80 GWh of renewables in March | Utility Dive.” [Online]. Available: http://www.utilitydive.com/news/caiso-california-curtailed-80-gwh-of-renewables-in-march/441078/. [Accessed: 27-Jul-2017].

[33] L. Bird *et al.*, “Wind and solar energy curtailment: A review of international experience,” *Renew. Sustain. Energy Rev.*, vol. 65, pp. 577–586, Nov. 2016.

[34] K. Strunz, E. Abbasi, and D. N. Huu, “DC Microgrid for Wind and Solar Power Integration,” *IEEE J. Emerg. Sel. Top. Power Electron.*, vol. 2, no. 1, pp. 115–126, Mar. 2014.

[35] J. R. Agüero and A. Khodaei, “Grid Modernization, DER Integration and Utility Business Models – Trends and Challenges,” p. 10, 2018.

[36] M. N. Faqiry and S. Das, “Double-Sided Energy Auction in Microgrid: Equilibrium Under Price Anticipation,” *IEEE Access*, vol. 4, pp. 3794–3805, 2016.

[37] Y. K. Renani, M. Ehsan, and M. Shahidehpour, “Optimal Transactive Market Operations With Distribution System Operators,” *IEEE Trans. Smart Grid*, vol. 9, no. 6, pp. 6692–6701, Nov. 2018.

[38] New York State Department of Public Service, “Developing the REV Market in New York: DPS Staff Straw Proposal on Track One Issues,” 2014.

[39] L. Kristov and P. De Martini, “21 st Century Electric Distribution System Operations,” 2014.

[40] G. Bade, “Chicago’s REV: How ComEd is reinventing itself as a smart energy platform | Utility Dive,” 2016. [Online]. Available: https://www.utilitydive.com/news/chicagos-rev-how-comed-is-reinventing-itself-as-a-smart-energy-platform/416623/. [Accessed: 28-Jan-2019].

[41] Z. Wang, B. Chen, J. Wang, M. M. Begovic, and C. Chen, “Coordinated Energy Management of Networked Microgrids in Distribution Systems,” *IEEE Trans. Smart Grid*, vol. 6, no. 1, pp. 45–53, Jan. 2015.

[42] S. Parhizi, A. Khodaei, and M. Shahidehpour, “Market-Based Versus Price-Based Microgrid Optimal Scheduling,” *IEEE Trans. Smart Grid*, vol. 9, no. 2, pp. 615–623, Mar. 2018.

[43] J. Tong and J. Wellinghoff, “Rooftop Parity: Solar for Everyone, Including Utilities,” *Public Utility Fortnightly*, pp. 18–23, Aug-2014.

[44] S. Bahramirad, A. Khodaei, and R. Masiello, “Distribution Markets,” *IEEE Power Energy Mag.*, vol. 14, no. 2, pp. 102–106, Mar. 2016.

[45] A. Alanazi, H. Babazadeh, and A. Khodaei, “Power Fluctuation Reduction in Wind Turbine Generator Systems,” in *North American Power Symposium*, Denver, CO, 2016, pp. 1–5.

[46] A. Alanazi and A. Khodaei, “Optimal Battery Energy Storage Sizing for Reducing Wind Generation Curtailment,” in *IEEE PES General Meeting, Chicago, IL*, 2017.

[47] P. Denholm *et al.*, *The impact of wind and solar on the value of energy storage*. National Renewable Energy Laboratory, 2013.

[48] S. Gill, G. W. Ault, and I. Kockar, “The optimal operation of energy storage in a wind power curtailment scheme,” in *2012 IEEE Power and Energy Society General Meeting*, 2012, pp. 1–8.

[49] S. Bahramirad, W. Reder, and A. Khodaei, “Reliability-Constrained Optimal Sizing of Energy Storage System in a Microgrid,” *IEEE Trans. Smart Grid*, vol. 3, no. 4, pp. 2056–2062, Dec. 2012.

[50] I. Alsaidan, A. Khodaei, and W. Gao, “Determination of Battery Energy Storage Technology and Size for Standalone Microgrids,” in *IEEE PES General Meeting*, Boston, MA, 2016, pp. 1–5.

[51] A. Alanazi, A. Khodaei, M. Chamana, and D. Kushner, “Wind Generation Curtailment Reduction based on Uncertain Forecasts,” in *CIGRE Grid of the Future Symposium*, Cleveland, OH, 2017.

[52] A. Khodaei, S. Bahramirad, and M. Shahidehpour, “Microgrid planning under uncertainty,” *IEEE Trans. Power Syst.*, vol. 30, no. 5, pp. 2417–2425, 2015.

[53] I. Alsaidan, A. Khodaei, and W. Gao, “Distributed Energy Storage Sizing for Microgrid Applications,” in *2016 IEEE/PES Transmission and Distribution Conference and Exposition (T&D)*, Dallas, TX, 2016, pp. 1–5.

[54] K. C. Divya and J. Østergaard, “Battery energy storage technology for power systems—An overview,” *Electr. Power Syst. Res.*, vol. 79, no. 4, pp. 511–520, Apr. 2009.

[55] "Microgrid Workshop Report August 2011.pdf." [Online]. Available: http://energy.gov/sites/prod/files/Microgrid%20Workshop%20Report%20August%202011.pdf. [Accessed: 22-Jan-2015].

[56] R. H. Lasseter, "Microgrids," in *Power Engineering Society Winter Meeting, 2002. IEEE*, 2002, vol. 1, pp. 305–308.

[57] A. Banerji *et al.*, "Microgrid: A review," in *Global Humanitarian Technology Conference: South Asia Satellite (GHTC-SAS), 2013 IEEE*, 2013, pp. 27–35.

[58] R. H. Lasseter and P. Paigi, "Microgrid: a conceptual solution," in *Power Electronics Specialists Conference, 2004. PESC 04. 2004 IEEE 35th Annual*, 2004, vol. 6, pp. 4285–4290.

[59] T. Logenthiran and D. Srinivasan, "Formulation of unit commitment (UC) problems and analysis of available methodologies used for solving the problems," in *Sustainable Energy Technologies (ICSET), 2010 IEEE International Conference on*, 2010, pp. 1–6.

[60] A. Khodaei, "Microgrid Optimal Scheduling With Multi-Period Islanding Constraints," *IEEE Trans. Power Syst.*, vol. 29, no. 3, pp. 1383–1392, May 2014.

[61] A. Khodaei, "Provisional Microgrids," *IEEE Trans. Smart Grid*, vol. 6, no. 3, pp. 1107–1115, May 2015.

[62] A. Khodaei, "Resiliency-Oriented Microgrid Optimal Scheduling," *IEEE Trans. Smart Grid*, vol. 5, no. 4, pp. 1584–1591, Jul. 2014.

[63] A. Alanazi, M. Alanazi, and A. Khodaei, “Managing the microgrid net load variability,” in *Transmission and Distribution Conference and Exposition (T&D), 2016 IEEE/PES*, 2016, pp. 1–5.

[64] “Levelized cost and levelized avoided cost of new generation resources in the Annual Energy Outlook 2014 - electricity_generation.pdf.” [Online]. Available: http://www.eia.gov/forecasts/aeo/pdf/electricity_generation.pdf. [Accessed: 14-May-2015].

[65] K. Lummi, A. Rautiainen, L. Peltonen, S. Repo, P. Jarventausta, and J. Rintala, “Microgrids as Part of Electrical Energy System - Pricing Scheme for Network Tariff of DSO,” in *2018 15th International Conference on the European Energy Market (EEM)*, 2018, pp. 1–5.

[66] S. Chen *et al.*, “Forming Bidding Curves for a Distribution System Operator,” *IEEE Trans. Power Syst.*, vol. 33, no. 5, pp. 5389–5400, Sep. 2018.

[67] M. H. S. Boloukat and A. A. Foroud, “Multiperiod Planning of Distribution Networks Under Competitive Electricity Market With Penetration of Several Microgrids, Part I: Modeling and Solution Methodology,” *IEEE Trans. Ind. Inform.*, vol. 14, no. 11, pp. 4884–4894, Nov. 2018.

[68] R. Mohammadi, H. R. Mashhadi, and M. Shahidehpour, “Market-based Customer Reliability Provision in Distribution Systems Based on Game Theory: A Bi-level Optimization Approach,” *IEEE Trans. Smart Grid*, pp. 1–1, 2018.

[69] A. Soroudi, M. Ehsan, R. Caire, and N. Hadjsaid, “Hybrid immune-genetic algorithm method for benefit maximisation of distribution network operators and

distributed generation owners in a deregulated environment," *IET Gener. Transm. Distrib.*, vol. 5, no. 9, p. 961, 2011.

[70] S. M. Sajjadi, P. Mandal, T.-L. B. Tseng, and M. Velez-Reyes, "Transactive energy market in distribution systems: A case study of energy trading between transactive nodes," in *2016 North American Power Symposium (NAPS)*, 2016, pp. 1–6.

[71] B. Illing, S. Naumann, S. Klaiber, and O. Warweg, "Market Scenarios for Integration of Distribution System Operators within the Scheduling System," in *2018 15th International Conference on the European Energy Market (EEM)*, 2018, pp. 1–5.

[72] A. Saint-Pierre and P. Mancarella, "Active Distribution System Management: A Dual-Horizon Scheduling Framework for DSO/TSO Interface Under Uncertainty," *IEEE Trans. Smart Grid*, vol. 8, no. 5, pp. 2186–2197, Sep. 2017.

[73] U. Markovic, E. Kaffe, D. Mountouri, F. Kienzle, S. Karagiannopoulos, and A. Ulbig, "The future role of a dso in distribution networks with high penetration of flexible prosumers," in *CIRED Workshop 2016*, 2016, pp. 175 (4 .)-175 (4 .).

[74] A. Mohammadi, M. Mehrtash, and A. Kargarian, "Diagonal Quadratic Approximation for Decentralized Collaborative TSO+DSO Optimal Power Flow," *IEEE Trans. Smart Grid*, pp. 1–1, 2018.

[75] A. Esmat and J. Usaola, "DSO congestion management using demand side flexibility," in *CIRED Workshop 2016*, 2016, pp. 197 (4 .)-197 (4 .).

[76] B. Mattlet and J.-C. Maun, “Assessing the benefits for the distribution system of a scheduling of flexible residential loads,” in *2016 IEEE International Energy Conference (ENERGYCON)*, 2016, pp. 1–6.

[77] S. Huang, Q. Wu, L. Cheng, Z. Liu, and H. Zhao, “Uncertainty Management of Dynamic Tariff Method for Congestion Management in Distribution Networks,” *IEEE Trans. Power Syst.*, vol. 31, no. 6, pp. 4340–4347, Nov. 2016.

[78] D. Koraki, J. Keukert, and K. Strunz, “Congestion management through coordination of distribution system operator and a virtual power plant,” in *2017 IEEE Manchester PowerTech*, 2017, pp. 1–6.

[79] C. Deckmyn, J. Van de Vyver, T. L. Vandoorn, B. Meersman, J. Desmet, and L. Vandevelde, “Day-ahead unit commitment model for microgrids,” *IET Gener. Transm. Distrib.*, vol. 11, no. 1, pp. 1–9, Jan. 2017.

[80] R. C. G. Teive *et al.*, “Intelligent system for automatic performance evaluation of distribution system operators,” in *2017 19th International Conference on Intelligent System Application to Power Systems (ISAP)*, 2017, pp. 1–6.

[81] E. A. C. A. Neto *et al.*, “A multicriteria approach for performance evaluation of distribution system operators,” in *2016 IEEE PES Transmission & Distribution Conference and Exposition-Latin America (PES T&D-LA)*, 2016, pp. 1–7.

[82] S. Gheorghe and C. Stanescu, “Performance of services achieved by transmission and distribution system operators in Romanian power grid,” in *2016 International Conference on Development and Application Systems (DAS)*, 2016, pp. 121–125.

[83] D. Apostolopoulou, S. Bahramirad, and A. Khodaei, “The Interface of Power: Moving Toward Distribution System Operators,” *IEEE Power Energy Mag.*, vol. 14, no. 3, pp. 46–51, May 2016.

[84] W. Becker, M. Hable, M. Malsch, T. Stieger, and F. Sommerwerk, “Reactive power management by distribution system operators concept and experience,” *CIRED - Open Access Proc. J.*, vol. 2017, no. 1, pp. 2509–2512, Oct. 2017.

[85] G. Ferro, R. Minciardi, M. Robba, and M. . Rossi, “Optimal voltage control and demand response: Integration between Distribution System Operator and microgrids,” in *2017 IEEE 14th International Conference on Networking, Sensing and Control (ICNSC)*, 2017, pp. 435–440.

[86] H. Lotfi and A. Khodaei, “Static hybrid AC/DC microgrid planning,” in *2016 IEEE Power & Energy Society Innovative Smart Grid Technologies Conference (ISGT)*, 2016, pp. 1–5.

[87] A. Alanazi, H. Lotfi, and A. Khodaei, “Coordinated AC/DC microgrid optimal scheduling,” in *2017 North American Power Symposium (NAPS)*, 2017, pp. 1–6.

[88] M. Alturki, A. Khodaei, A. Paaso, and S. Bahramirad, “Optimization-based distribution grid hosting capacity calculations,” *Appl. Energy*, vol. 219, pp. 350–360, Jun. 2018.

[89] H. Lotfi and A. Khodaei, “AC Versus DC Microgrid Planning,” *IEEE Trans. Smart Grid*, vol. 8, no. 1, pp. 296–304, Jan. 2017.

[90] “CPLEX 12.” [Online]. Available: https://www.gams.com/latest/docs/S_CPLEX.html. [Accessed: 17-Dec-2018].

List of Publications:

- **A. Alanazi**, H. Lotfi and A. Khodaei, "Market Clearing in Microgrid-Integrated Active Distribution Networks," Submitted to Electric Power System Research.
- **A. Alanazi**, and A. Khodaei, "Impact of Grid Reconfiguration in Distribution Market Clearing and Settlement," CIGRE Grid of the Future Symposium, Reston, VA, October 2018.
- **A. Alanazi**, H. Lotfi and A. Khodaei, " Optimal Energy Storage Sizing and Siting in Hybrid AC/DC Microgrids," North American Power Symposium, Fargo, ND, September 2018.
- I. Alsaidan, **A. Alanazi**, W. Gao, H. Wu, and A. Khodaei, "State-Of-The-Art in Microgrid-Integrated Distributed Energy Storage Sizing," *Energies*, vol. 10, no. 12, p. 1421, September 2017.
- **A. Alanazi**, A. Khodaei, M. Chamana, and D. Kushner, "Wind Generation Curtailment Reduction based on Uncertain Forecasts," CIGRE Grid of the Future Symposium, Cleveland, OH, October 2017.
- **A. Alanazi**, H. Lotfi and A. Khodaei, "Coordinated AC/DC Microgrid Optimal Scheduling," North American Power Symposium, Morgantown, WV, September 2017.
- **A. Alanazi**, and A. Khodaei, "Optimal Battery Energy Storage Sizing for Reducing Wind Generation Curtailment," IEEE PES General Meeting, Chicago, IL, July 2017.
- **A. Alanazi**, H. Babazadeh, and A. Khodaei, "Power Fluctuation Reduction in Wind Turbine Generator Systems," North American Power Symposium, Denver, CO, September 2016.
- **A. Alanazi**, M. Alanazi, and A. Khodaei, "Managing the Microgrid Net Load Variability," IEEE PES Transmission and Distribution Conference, Dallas, TX, May 2016.
- M. Alanazi, **A. Alanazi**, and A. Khodaei, "Long-Term Solar Generation Forecasting," IEEE PES Transmission and Distribution Conference, Dallas, TX, May 2016.